Journal of Structural Geology 32 (2010) 1960–1977

Contents lists available at ScienceDirect

Journal of Structural Geology

journal homepage: www.elsevier.com/locate/jsg

Determining brittle extension and shear strain using fault-length and displacement systematics: Part I: Theory

Robert J. Twiss [a,*], Randall Marrett [b]

[a] Geology Department, University of California at Davis, One Shields Ave., Davis, CA 95616-8605, USA
[b] Department of Geological Sciences, Jackson School of Geosciences, University of Texas at Austin, 1 University Station C1100, Austin, TX 78712-0254, USA

ARTICLE INFO

Article history:
Received 25 April 2009
Received in revised form
2 April 2010
Accepted 12 April 2010
Available online 25 May 2010

Keywords:
Brittle deformation
Strain
Extension
Shear strain
Fault systematics
Fault scaling

ABSTRACT

We derive the exact equations by which the continuum approximation to the extensional and shear strains can be determined from measurements of fault-lengths or fault-displacement in a faulted domain. We develop the theory by which we can infer the extensional and shear strain in a volume of brittlely deformed crust from an incomplete inventory of the faults. To that end, we use empirical power-law relationships between fault-length and fault-displacement, and the power-law cumulative frequency distribution for each of these variables, for sampling domains of one, two, and three dimensions. The theory 1) defines the relationships among the parameters in these power-laws, which allows the self-consistency of results from fault-length and fault-displacement studies in domains of one, two, and three dimensions to be evaluated; 2) defines constraints on the relative sizes of the sampling domain and the largest fault that can be included in an analysis using fault systematics; 3) shows that extensional and shear strains in faulted crust can be inferred knowing only an independent set of the parameters defining the population systematics plus the magnitude of either the displacement or the length for the largest fault in the domain; and 4) defines the constraints on the three-dimensional strain imposed by sampling in one- and two-dimensional domains.

1. Introduction

The sizes of faults span a tremendous range — so wide a range, in fact, that no single approach for observation could hope to achieve a complete inventory. It is observed empirically, however, that the abundance of faults as a function of fault-length is described by a power-law relationship, with the frequency of faults increasing exponentially as their size decreases (e.g., Scholz and Cowie, 1990; Walsh et al., 1991; Marrett and Allmendinger, 1992; Cladouhos and Marrett, 1996; Watterson et al., 1996; Marrett et al., 1999; Bonnet et al., 2001). Moreover, fault-displacement decreases systematically as fault-length decreases (e.g. Marrett and Allmendinger, 1991; Clark and Cox, 1996). As a consequence, although small faults individually contribute less than do large faults to strain and other bulk physical characteristics of the faulted volume of rock, their high abundance may compensate for their small individual contribution.

Power-law distributions of fault sizes provide both obstacles and opportunities for addressing problems that inherently depend on populations of faults. For example, the magnitude of deformation due to faulting may depend not just on the largest faults, but rather on all faults of all sizes contained in a domain of interest, and available sampling of the faults is commonly insufficient to provide accurate estimates of the deformation. However, if data are lacking on the full range of fault sizes, the phenomenon of fault scaling provides a tool with which we may quantify statistically the contribution of the unobserved categories of faults. For current purposes, we limit attention to scaling of fault-lengths and displacements, as opposed to topological scaling of fault network geometry (e.g., via box counting; Walsh and Watterson, 1993). In this contribution we focus on fault-related strain, but analogous problems include permeability of fractured rock (recently reviewed by Molz et al., 2004), which can limit the rate of fluid flow; and fracture surface area, which can limit the rate of chemical interaction between fluids and rock (Marrett, 1996).

A review of empirical results pertaining to fault scaling was published recently (Bonnet et al., 2001), but we have lacked a complete theory by which these empirical results can be compared and evaluated. Previous fragments of theoretical work have been intentionally narrow in order to simplify the analysis, but this also has limited the scope of applicability and in some cases

* Corresponding author. Tel.: +1 530 752 0352/756 3326; fax: +1 530 752 0951.
E-mail addresses: rjtwiss@ucdavis.edu (R.J. Twiss), marrett@mail.utexas.edu (R. Marrett).

0191-8141/$ – see front matter © 2010 Elsevier Ltd. All rights reserved.
doi:10.1016/j.jsg.2010.04.007

has led to confusion. For example, Scholz and Cowie (1990) inferred that small faults contribute negligible strain, but their conclusions were potentially undercut by having applied fault data sampled in a two-dimensional domain to a three-dimensional problem without stereological correction.

In this paper, we begin with first principles and derive a full and systematic theory for the application of fault scaling relations to the inference of fault-related extensional and shear strain for one-, two-, and three-dimensional domains that have been deformed by a large population of homogeneously distributed faults. A brief summary of part of this development for extension in three dimensions was published in Twiss and Moores (2007; Box 16-I, p. 440). We first derive the equations by which the continuum approximation of extensional and shear strain in a domain can be determined from displacements on a set of faults that deform the domain. We then adopt empirical power-law equations that relate fault-length to fault-displacement and that define the cumulative frequency distributions of faults as a function of each of these two variables. Different equations for cumulative frequency apply to data sampled in one-, two-, and three-dimensional domains, and heretofore, the relationships among these equations have not been clear. We show that the parameters in these equations are not all independent, and we derive the relationships among them.

Implicit in the use of fault systematics to determine strain in a domain is an assumption that the faults are homogeneously distributed throughout the domain and that the domain is large relative to the size of the faults. We derive the size constraints that define, for a given size of domain, the largest fault that can be included in the analysis, or conversely, the minimum size of the domain that must be used to incorporate a given maximum-sized fault in the analysis.

If we know a set of independent parameters that define the fault systematics in a faulted domain, the theory shows that both extensional and shear strains can be inferred from either the displacement on, or length of, the largest fault in the domain. Heretofore, it has not been clearly recognized that determinations of strain based on sampling in one- or two-dimensional domains do not necessarily define the three-dimensional strain exactly; nevertheless, they at least place constraints on it, and we derive equations that specify those constraints.

The question, "Are small faults important?" has contradictory answers in the literature (e.g., Scholz and Cowie, 1990; Walsh et al., 1991; Marrett and Allmendinger, 1991, 1992), due in part to theoretical confusion and in part to semantics. In this paper, small faults are defined to be one order of magnitude or more smaller than the largest fault that can be included in the analysis for the domain under study, without regard to absolute scale (Walsh et al., 1991; Marrett and Allmendinger, 1992). We derive the relation between the size of the largest fault and the size of the domain in Section 3.4. In particular, we do not adopt the definition, used for example by Scholz and Cowie (1990), that small faults are those that do not span the brittle crust. Our results show that relatively small faults contribute significantly to the total strain in a brittlely deformed volume.

In a companion paper (Twiss and Marrett, in this issue, referred to as Part II), we use the theoretical results to compare and evaluate multiple sets of data from the same domains, and we use empirical data to calculate the extensional strains for these areas and to test the predictions of the theory. Figure and equation references with numbers that begin with a "II:" refer to this companion paper.

For ease of reference, all symbols used in the analysis are listed alphabetically in Table 1, along with a definition and the equation number of first use and/or occurrence that is relevant to the definition.

2. Continuum strains of faulted domains

2.1. Infinitesimal continuum extension from brittle faulting

The first problem we address is how to find the continuum approximation to the extension in a specific direction across a faulted terrane. We begin with the result for the calculation of the average infinitesimal constant volume strain tensor that results from the slip on a set of non-rotating faults within a volume $\mathcal{V}$ of rock, where $\mathcal{V}$ is large relative to the dimension of the largest fault contained in the volume. The strain of a volume $\mathcal{V}$ that is contributed by a single fault completely contained within the volume, is (Kostrov (1974), referencing Riznichenko (1965); see also Twiss (2009)).

$$e_{kl} = \frac{1}{2\mathcal{V}} M_0[\eta_k n_l + \eta_l n_k], \tag{2.1.1}$$

where η_k and n_k are the components of unit vectors parallel, respectively, to the slip direction and the normal to the fault (Fig. 1). The slip direction is defined by the motion of the fault block into which **n** points.

In Eq. (2.1.1), M_0 is the geometric moment defined by

$$M_0 = A\delta, \tag{2.1.2}$$

where A is the area of the fault over which the slip occurs, and δ is the mean of the displacement magnitudes over the fault surface. The geometric moment is similar to the scalar seismic moment except that the shear modulus, which is part of the definition of the seismic moment, is not included in the geometric moment. Twiss and coworkers have used continuum micropolar theory to account for the effects of rotating fault blocks on the slip directions and the geometric moment tensor (Twiss et al., 1991, 1993; Twiss, 2009), but we ignore those effects in this analysis.

Note that if $\boldsymbol{\delta}$ is the displacement vector for the block into which **n** points, and if the magnitude of the displacement is δ, then

$$\boldsymbol{\eta} \equiv \frac{\boldsymbol{\delta}}{|\boldsymbol{\delta}|} = \frac{\boldsymbol{\delta}}{\delta}, \quad \boldsymbol{\delta} = \delta\boldsymbol{\eta}. \tag{2.1.3}$$

The extension in the direction parallel to the unit vector **t** (Fig. 1) is determined from the strain tensor by

$$e_{(3,t)} = e_{kl} t_k t_l, \tag{2.1.4}$$

where, the subscript '(3,t)' on the symbol for the extension indicates that this expression applies to the extension of the three-dimensional domain $\mathcal{V}$ parallel to the unit vector **t**. We adopt the Einstein summation convention for repeated subscripts in any given term. We define the angle ϕ to be the angle between the slip direction $\boldsymbol{\eta}$ on the fault and the traverse direction **t**, and θ to be the angle between the normal to the fault plane **n** and the traverse direction **t** (Fig. 1) so that

$$\eta_k t_k = \cos\phi, \quad n_k t_k = \cos\theta, \tag{2.1.5}$$

Then we substitute for the strain tensor in Eq. (2.1.4) using Eqs. (2.1.1), (2.1.2), and (2.1.5), and write the result for the ith fault in a set of $N^{(\max)}$ faults,

$$e^{(i)}_{(3,t)} = \frac{A^{(i)} \cos\theta^{(i)} \delta^{(i)} \cos\phi^{(i)}}{\mathcal{V}}. \tag{2.1.6}$$

This equation gives the volumetric average of the extension in the direction **t** contributed by the ith fault in the volume $\mathcal{V}$. We can rewrite Eq. (2.1.6) in the form

Table 1
Notation.

Symbol	Definition or description	Eq. no. for definition or first use
A, $A^{(i)}$, $A_t^{(i)}$	- Area of a fault, or of the ith fault, over which the displacement occurs; subscript 't' indicates the projection of the area on a plane normal to **t**.	(2.1.2), (2.1.6), (2.1.13), (2.4.3)
$\mathcal{A}$, $\mathcal{A}_t = \mathcal{WH}$, $\mathcal{A}_w = \mathcal{TH}$, $\mathcal{A}_h = \mathcal{TW}$	- Cross-sectional area of the volume $\mathcal{V}$; subscripts indicate orientation of the area normal to the unit vector **t**, **w**, or **h**, respectively	(2.1.7), (2.1.9)
B	- Constant in the fault-length–fault-displacement relationship. $1/B$ defines the displacement on faults of unit length in any specific area. Dimensions of $[\text{length}]^{(p-1)}$	(3.1.1)
$C_{(\zeta,v)}$: $\zeta = 1, 2, 3$; $v = t, \perp h$	- Constants of integration.	(4.1.27)–(4.1.29), (4.1.32)–(4.1.34), (S1.2.2), (S1.2.6), (S2.3.2), (S2.3.7), (S3.4.2), (S3.4.7)
$D_{(\zeta,x)}$: $\zeta = 1, 2, 3$; $x = t, \gamma$	- A combination of constants in the equations for extension of material lines parallel to **t** ($x = t$), or shear strain of material lines parallel to **t** and **w** ($x = \gamma$) for a ζ-dimensional domain.	(4.1.11), (4.1.12), (4.1.14), (4.1.15)
$\boldsymbol{e_{kl}}$	- Strain tensor contributed by displacement on a single fault, averaged over a faulted domain $\mathcal{V}$, the dimensions of which are large relative to the fault.	(2.1.1)
$e_{(\zeta,x)}$, $e^{(i)}_{(\zeta,x)}$, $e^{(\text{cum})}_{(\zeta,x)}$, $e^{(\text{tot})}_{(\zeta,x)}$, $e^{(i)}_{(\zeta,\gamma v)}$: $\zeta = 1, 2, 3$; $x = t, \gamma$; $v = t, w$	- Extensional strain of in a ζ-dimensional domain parallel to either **t** ($x = t$) or **w** ($x = w$), or shear strain in a ζ-dimensional domain of the pair of orthogonal lines parallel to **t** and **w** ($x = \gamma$); no superscript refers to the total strain from one or more faults; superscript (i) indicates strain contributed by the ith fault; superscripts '(cum)', and '(tot)' indicate, respectively, the cumulative strain, and the total strain. The subscript 'γv' is the part of the shear strain for the line segment parallel to **t** (or **w**) ($v = t$ (or w)) relative to **w** (or **t**).	(2.1.4), (2.1.6), (2.1.12), (2.2.1), (2.2.4), (2.2.7), (4.1.1)–(4.1.6), (4.1.23)–(4.1.26), (4.1.36)–(4.1.39), (4.1.40)–(4.1.42)
$f_{(\zeta,v)}(L)$, $f_{(\zeta,v)}(\delta)$: $\zeta = 1, 2, 3$; $v = t, w, \perp h$	- Cumulative frequency of faults having length $\geq L$, or displacement $\geq \delta$, as determined by the sampling of a ζ-dimensional domain. Subscript v indicates the orientation of the sampling domain (omitted when $\zeta = 3$).	(3.1.4), (3.1.5), (3.1.8), (3.1.11), (3.1.13)
$G_{(\zeta,v)}$: $\zeta = 1, 2, 3$; $v = t, w, \perp h$	- Constant relating the cumulative number of faults to the fault-length; equals the cumulative number of faults having a unit length. When $\zeta = 3$, the subscript v is omitted. Units of $[(\text{km})^{m_\zeta}]$	(3.1.3), (3.1.5)
$g_{(\zeta,v)}$: $\zeta = 1, 2, 3$; $v = t, w, \perp h$	- Constant relating the cumulative frequency of faults to the fault-length; equals the cumulative frequency of faults having a unit length. When $\zeta = 3$, the subscript v is omitted. Units of $[(\text{km})^{m_\zeta}/(\text{km})^2]$	(3.1.4), (3.1.5)
$\mathcal{H}$, $\mathcal{H}_0$	- Vertical dimension of the sampling volume $\mathcal{V}$, parallel to the unit vector **h**, in the deformed and undeformed state, respectively.	(2.1.8), (2.1.9), (2.4.3), Fig. 2
h, h_k, $\perp h$	- Vertical unit vector, and its components, oriented perpendicular to **t** and **w**. $\perp h$ is used as a subscript ($v = \perp h$) to indicate a horizontal planar domain oriented perpendicular to **h**.	Fig. 2, (3.1.6)
i	- Superscript referring to the ith fault, for faults numbered from $i = 1{:}N^{(\max)}$ in order of decreasing length or displacement.	(2.1.6)
$K_{(1,v)}$: $v = t, w$	- Constants of integration for the cumulative shear strain determined by sampling along two orthogonal lines parallel, respectively, to **t** and **w**	(4.1.30), (4.1.35)
L, $L^{(i)}$	- Horizontal dimension of a fault, or of the ith fault, as measured in the sampling domain.	(2.1.13), (3.1.1)
l, $l^{(i)}$	- The down-dip width of a fault, or of the ith fault	(2.1.14), (3.1.21)
M_0	- The geometric moment for slip on a fault	(2.1.1), (2.1.2)
m_ζ	- Exponent on the fault-length in the power-law relation between cumulative number or cumulative frequency and fault-length, as determined by sampling of a ζ-dimensional domain.	(3.1.3)
$N_{(\zeta,v)}(L)$, $N_{(\zeta,v)}(\delta)$, $N_{(\zeta,v)}$: $\zeta = 1, 2, 3$; $v = t, w, \perp h$	- Cumulative number of faults having length $\geq L$, or displacement $\geq \delta$, as determined by sampling of a ζ-dimensional domain oriented as indicated by v. When $\zeta = 3$, v is not included in the subscript.	(3.1.3), (3.1.7), (3.1.15)
$N^{(\max)}$	- Total number of faults in a volume $\mathcal{V}$.	(2.1.12)
n, n_k	- Unit vector and its components normal to a fault surface.	(2.1.1)
${}_\zeta\mathcal{P}_v^{(i)}$: $\zeta = 1, 2, 3$; $v = t, w, \perp h$	- The probability that in a ζ-dimensional domain (left subscript), the ith fault (superscript) is intersected by a random line parallel to **t** or **w** ($v = t$ or w) or a plane perpendicular to **h** ($v = \perp h$) (right subscript).	(2.1.10), (2.2.5), (3.1.19), (3.1.20), (3.1.22), $(3.1.29)_{1,2}$, (4.1.1), (4.1.6), (4.1.7), (4.1.9)
${}_\zeta\mathcal{P}_v$: $\zeta = 1, 2, 3$; $v = t, w, \perp h$	- Continuous function (of length or displacement) defining the probability that a fault of a given length or displacement in a ζ-dimensional domain (left subscript) will be intersected by a randomly located lower-dimensional domain having an orientation v (right subscript); $v = t$ for one-dimensional domains parallel to **t**, or $v = \perp h$ for a two-dimensional domain perpendicular to **h**.	(3.1.15), (3.1.23), (3.1.24), $(3.1.29)_{3,4}$
${}_3\mathcal{P}_v$: $v = t, w, \perp h$	- Continuous function defined as the product of the probability ${}_3\mathcal{P}_v$ and the volume associated with a unit size of the domain ($\mathcal{V}/\mathcal{T}$ for $v = t$; $\mathcal{V}/\mathcal{A}_h$ for $v = \perp h$).	(3.1.16)–(3.1.18), (3.1.25), (3.1.26), (3.1.30)
p	- Exponent on the length in the relationship between fault-length and fault-displacement.	(3.1.1)
$R_{(\zeta,v)}$: $\zeta = 1, 2, 3$; $v = t, w, \perp h$	- Constant in the equation relating the cumulative number of faults to the displacement on the faults; equals the cumulative number of faults on which the displacement is of unit length. Subscript 'ζ' indicates dimension of the sampling domain; subscript 'v' indicates orientation of sampling domain (omitted when $\zeta = 3$). Units of $[(\text{length})^{s_\zeta}]$.	$(3.1.9)_{2,3}$, (3.1.10), (3.1.12)

Table 1 (*continued*)

Symbol	Definition or description	Eq. no. for definition or first use
$r_{(\zeta,v)}$: $\zeta = 1, 2, 3$; $v = t, w, \perp h$	- Constant in the equation relating the cumulative frequency of faults and the displacement on the faults; equals the cumulative frequency of faults on which the displacement is of unit length. Subscript 'ζ' indicates dimension of the sampling domain; subscript 'v' indicates orientation of sampling domain (omitted when $\zeta = 3$). Units of $[(\text{length})^{s_\zeta}/(\text{length})^{\zeta}]$.	$(3.1.9)_3$, (3.1.11), (3.1.12)
s_ζ	- Exponent on the displacement in the power-law relation between cumulative number or cumulative frequency and fault-displacement, as determined by sampling of a ζ-dimensional domain.	$(3.1.9)_1$, (3.1.10), (3.1.11)
$\mathcal{T}$, $\mathcal{T}_0$	- The deformed and undeformed lengths of the horizontal material line that is the dimension of the volume $\mathcal{V}$ parallel to **t**. They are approximately equal in the infinitesimal strain approximation.	(2.1.8), (2.1.9), (2.1.11)
$\Delta\mathcal{T}_v^{(i)}$: $v = t, w$	- Displacement in the direction **t** or **w** ($v = t$ or w) contributed by the ith fault intersected by the sampling line parallel to **t** or **w.**	(2.3.1), (S3.3.2), $(S3.3.3)_{1,3}$
t, t_k	- Horizontal unit vector, and its components, parallel to the traverse direction in which the extension or shear strain is determined (normal to the unit vector **w**)	(2.1.4)
U_k	- Continuum displacement vector components.	(S3.3.1)
$\mathcal{V}$, $\mathcal{V}_0$	- The deformed and undeformed volume of rock for which the strain is determined, having deformed or undeformed dimensions, respectively, of [length, width, height] $= [\mathcal{T}, \mathcal{W}, \mathcal{H}]$ or $[\mathcal{T}_0, \mathcal{W}_0, \mathcal{H}_0]$.	(2.1.1), (2.1.8)
v	- As a subscript, it stands for subscripts that define the orientation of a domain, e.g. $v = t$ or w for lines parallel to **t** or **w**; or $v = \perp h$ for horizontal planes normal to **h**. In the companion paper, Part II, it represents the maximum throw on a fault (the vertical component of the displacement).	(3.1.3), (3.1.4), (II:2.6)
$\mathcal{W}$, $\mathcal{W}_0$	- The deformed and undeformed length of a horizontal material line that is the dimension of the volume $\mathcal{V}$ parallel to **w** and normal to **t**. They are approximately equal in the infinitesimal strain approximation.	(2.1.8), (2.1.9), (2.4.3)
$\Delta\mathcal{W}_t^{(i)}$	- The displacement parallel to **w** due to slip on the ith fault intersected by the sampling line parallel to **t**.	(S3.3.2), $(S3.3.3)_2$
w, w_k	- Horizontal unit vector, and its components, perpendicular to both **t** and **h**.	(2.2.1), Fig. 1
x	- Subscript that stands for both t and γ; used as a condensed notation in equations that have the same form for both extensional and shear strain.	(4.1.11), (4.1.12)
$\alpha^{(i)}$, α	- Angle between the direction **w** (which is normal to the horizontal line **t**) and the fault plane normal **n**; superscript '(i)' indicates the ith fault; no superscript applies to all faults assumed to have the same orientation.	(2.2.2), (2.2.3), (2.1.16), Fig. 1A
$\beta^{(i)}$, β	- Angle between the horizontal direction **w** (which is normal to the horizontal line **t**) and the fault-slip direction **η**; superscript '(i)' indicates the ith fault; no superscript applies to all faults assumed to have the same orientations of fault plane and slip direction.	(2.2.2), (2.2.3), (2.1.16), Fig. 1A
$\Delta_{(\zeta,v)}$: $\zeta = 1, 2, 3$; $v = t, w, \perp h$	- The size of the ζ-dimensional sampling domain; for $\zeta = 3$, it is the volume $\mathcal{V}$ of the domain; for $\zeta = 2$, it is the area $\mathcal{A}_h = \mathcal{T}\mathcal{W}$ of a horizontal plane through that volume; for $\zeta = 1$, it is the length $\mathcal{T}$ or $\mathcal{W}$ of a horizontal traverse across that volume; subscript v indicates the orientation of the sampling domain parallel to **t**, **w**, or normal to **h** (not used for $\zeta = 3$).	(3.1.5), (3.1.6)
δ	- Fault-displacement vector (which is parallel to the unit vector **η**).	(2.1.3)
δ, $\delta^{(i)}$,$\delta^{(\max)}_{(\zeta,v)}$: $\zeta = 1, 2, 3$; $v = t, w, \perp h$	- Magnitude of the mean displacement on a fault (superscript (i) indicates the ith fault). When $i = 1$, the displacement is for the largest-displacement fault in the ζ-dimensional sampling domain (superscript '(max)'); v indicates the orientation of the domain parallel to the unit vectors **t** or **w** ($v = t$ or w) or perpendicular to **h** ($v = \perp h$).	(2.1.2), (2.1.3), (2.1.6), (3.3.1)–(3.3.4), (4.1.31),
$\varepsilon^{(i)}$, ε	- The angle between ξ (which is the orthogonal projection onto a horizontal plane of the unit normal **n** to a fault) and the unit vector **w**. The angle lies in the horizontal plane that is normal to **h**; superscript '(i)' indicates the ith fault; no superscript applies to all faults assumed to have the same orientation.	Fig. 1B (2.1.16), $(S2.1.8)_2$,
$\phi^{(i)}$, ϕ	- Angle between the horizontal direction **t** and the slip direction **η** on a fault; superscript '(i)' indicates the ith fault; no superscript applies to all faults, assumed to have the same fault and slip orientations.	Fig. 1A (2.1.5), (2.1.6), (2.1.16),
γ	- Subscript used to imply shear strain of material lines that are parallel to the orthogonal unit vectors **t** and **w**.	(2.2.1)
η, η_k	- Unit vector and its components parallel to the fault-displacement for the fault-block into which the fault-normal **n** points.	(2.1.1), (2.1.3)
$\kappa^{(i)}$, κ	- The angle between ξ (which is the orthogonal projection onto a horizontal plane of the unit normal **n** to a fault) and the unit vector **t**. The angle lies in the horizontal plane normal to **h**; superscript '(i)' indicates the ith fault; no superscript applies to all faults, assumed to have the same orientation.	Fig. 1B (2.1.16), $(S2.1.8)_1$,
$\lambda^{(i)}$, λ	- Geometrical shape factor for a fault that accounts for the ratio of the down-dip width to the length, and for the shape of the fault tip line; superscript '(i)' indicates the ith fault; no superscript applies to all faults, assumed to have the same geometry.	(2.1.13), (2.1.14), (S2.2.8)

(*continued on next page*)

Table 1 (*continued*)

Symbol	Definition or description	Eq. no. for definition or first use
$\mu^{(i)}$, μ	The ratio of the down-dip width l of a fault to its length L; superscript '(i)' indicates the ith fault; no superscript applies to all faults, assumed to have the same geometry.	(3.1.20), (3.1.21), (S2.2.8)
$\nu^{(i)}$, ν	- The ratio of the average length of the fault trace on random horizontal planes, to the maximum length of the fault parallel to the plane. It accounts for the effect of the shape of the fault tip line on the length of the fault trace on a horizontal plane. Superscript '(i)' indicates the ith fault; no superscript applies to all faults, assumed to have the same geometry.	(4.1.10), (2.1.16), (S2.1.18), (S2.2.8)
$\rho^{(i)}$, ρ	- The dip of a fault; superscript '(i)' indicates the ith fault; no superscript applies to all faults, assumed to have the same orientation.	Fig. 1B, (3.1.20), (2.1.16)
$\theta^{(i)}$, θ	- Angle between the normal **n** to a fault plane, and the direction **t**; superscript '(i)' indicates the ith fault; no superscript applies to all faults, assumed to have the same orientation.	Fig. 1A, $(2.1.5)_2$, (2.1.6), (2.1.16)
$\xi^{(i)}$, $\xi_k^{(i)}$	- The normal to the trace of the ith fault within the horizontal two-dimensional sampling domain that is perpendicular to **h**; it is the orthogonal projection of the fault normal $\mathbf{n}^{(i)}$ onto the sampling domain. *Not* a unit vector.	Fig. 1B, (S2.1.5), (S2.1.7)
ψ	- Shear angle; tensor shear strain = 0.5 tan ψ	Fig. 2B, (2.4.2)
ζ	- Subscript indicating the number of spatial dimensions in a sampling domain.	(3.1.3), (3.1.4)

Symbols used in the paper are listed alphabetically, first for the Roman alphabet, then for the Greek alphabet.
Equation numbers beginning with "S" refer to the Supplementary Material available on line.

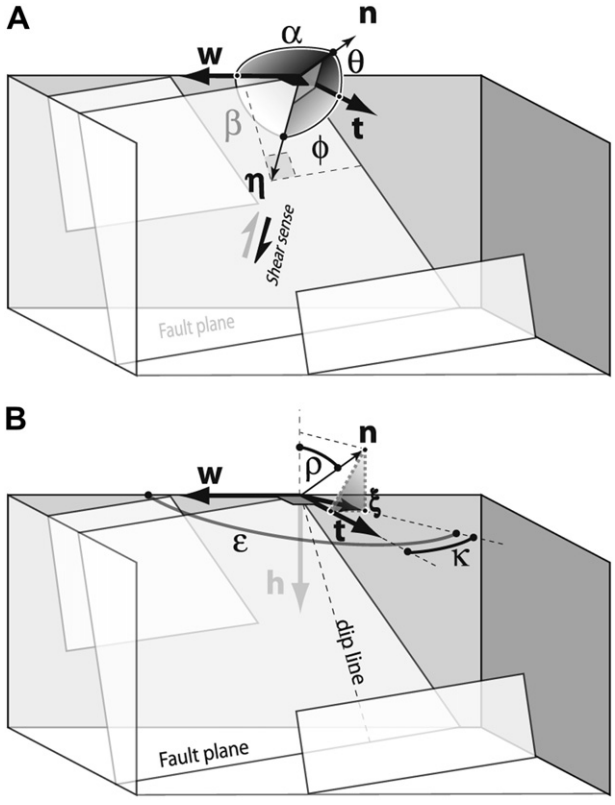

Fig. 1. Geometry for the fault-slip analysis showing three parallel fault planes of different sizes cutting the volume. Vectors and angles used in the analysis are illustrated. A. **n** is the unit normal to the fault plane, and it points into the fault block whose displacement direction is parallel to the unit vector **η**. The direction in which we determine the extension is parallel to the unit vector **t**, and the direction relative to which material lines parallel to **t** are sheared is defined by the unit vector **w**, which is orthogonal to **t**. B. **n**, **t**, and **w** are the same as in part A. **h** is a unit vector that is vertical pointing down. **ξ** is a vector that is the projection of **n** onto the horizontal surface. It is not a unit vector.

$$e^{(i)}_{(3,t)} = \left[\frac{A^{(i)}\cos\theta^{(i)}}{\mathcal{A}_t}\right]\left[\frac{\delta^{(i)}\cos\phi^{(i)}}{\mathcal{T}}\right], \tag{2.1.7}$$

where we define the linear dimensions of the specified volume after deformation to be $\mathcal{V}$, $\mathcal{W}$, and $\mathcal{H}$, which are parallel, respectively, to the orthogonal triad of unit vectors **t**, **w**, and **h**. Westaway (1994) also used Kostrov's results as a starting point for his analysis but did not use Eq. (2.1.4) and thus found a different result from Eq. (2.1.6). For convenience, we consider **t** and **w** to be horizontal and **h** to be vertical, although those orientations are not required. We define the cross-sectional areas of $\mathcal{V}$ normal to those unit vectors as follows (Fig. 2A):

$$\mathcal{V} \equiv \mathcal{T}\,\mathcal{W}\,\mathcal{H}, \tag{2.1.8}$$

$$\mathcal{A}_t \equiv \frac{\mathcal{V}}{\mathcal{T}} = \mathcal{W}\mathcal{H}, \quad \mathcal{A}_w \equiv \frac{\mathcal{V}}{\mathcal{W}} = \mathcal{T}\mathcal{H}, \quad \mathcal{A}_h \equiv \frac{\mathcal{V}}{\mathcal{H}} = \mathcal{T}\mathcal{W}. \tag{2.1.9}$$

In Eq. (2.1.7), the first term in brackets is the ratio of the fault area projected onto a plane normal to **t**, to the cross-sectional area of the averaging volume $\mathcal{V}$, where the cross section is also normal to **t** (Eq. $(2.1.9)_1$). This ratio, therefore, is just the probability ${}_3\mathfrak{P}_t^{(i)}$ that in a three-dimensional domain $\mathcal{V}$ (left subscript), the ith fault (superscript) is intersected by a random line parallel to **t** (right subscript),

$${}_3\mathfrak{P}_t^{(i)} \equiv \frac{A^{(i)}\cos\theta^{(i)}}{\mathcal{V}/\mathcal{T}} = \frac{A^{(i)}\cos\theta^{(i)}}{\mathcal{A}_t}. \tag{2.1.10}$$

The second term in brackets in Eq. (2.1.7) is the component of the slip in the direction of the sampling line, divided by the length $\mathcal{T}$ of that line. If we make the infinitesimal strain assumption that the deformed and undeformed lengths of the sampling line are the same, to a first order approximation, then

$$\mathcal{T} \approx \mathcal{T}_0, \tag{2.1.11}$$

and this term is just the local extension parallel to **t** due to slip on the ith fault. Thus, Eq. (2.1.7) shows that the contribution of the ith fault to the total extension parallel to **t** of the volume $\mathcal{V}$ is just the ith local extension in that direction (second term in Eq. (2.1.7)) scaled by the size (area) of the ith fault relative to the cross-

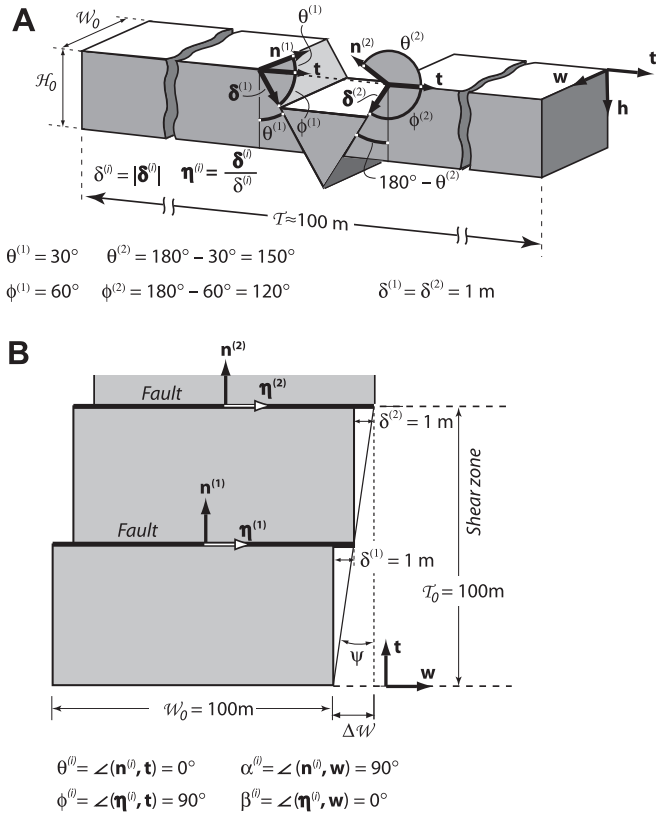

Fig. 2. Examples of strain components for blocks cut by simple sets of faults. A. Extension of a block of length $\mathcal{T}$, height $\mathcal{H}_0$, and width $\mathcal{W}_0$ cut by a pair of conjugate normal faults. $\mathbf{n}^{(i)}$ $(i = 1, 2)$ are unit vectors normal to the two fault planes, and $\mathbf{t}$ is a unit vector parallel to the direction in which the extension is determined. $\boldsymbol{\delta}^{(i)}$ $(i = 1, 2)$ are the displacement vectors on the two fault planes; they are parallel to the unit vectors $\boldsymbol{\eta}^{(i)}$ $(i = 1, 2)$. B. Shear strain of a line parallel to $\mathbf{t}$ relative to a line parallel to $\mathbf{w}$ in a block of height $\mathcal{T}_0$, width $\mathcal{W}_0$, and thickness $\mathcal{H}_0$ normal to the diagram (not shown). The block is cut by two parallel strike-slip faults. Vectors are defined as in Part A. $\delta^{(i)} = |\boldsymbol{\delta}^{(i)}|$ is the magnitude of the displacement vector.

sectional area of the volume, and by its orientation relative to $\mathbf{t}$ (first term in Eq. (2.1.7)); this scaling factor is just the probability defined in Eq. (2.1.10).

The total continuum extension of the volume $\mathcal{V}$ is just the sum over all $N^{(\max)}$ faults in the volume, of the weighted local extensions contributed by each fault in the system,

$$e^{(\mathrm{tot})}_{(3,t)} = \sum_{i=1}^{N^{(\max)}} e^{(i)}_{(3,t)} = \sum_{i=1}^{N^{(\max)}} \frac{A^{(i)}\delta^{(i)}}{\mathcal{V}} \cos\theta^{(i)} \cos\phi^{(i)}. \tag{2.1.12}$$

For this summation, we assume the faults are ordered by displacement from the largest, for which $i = 1$, down to the smallest, for which $i = N^{(\max)}$, so that if we sum over $i = 1{:}N$ faults, where $N < N^{(\max)}$, we obtain the cumulative contribution to the extension by the N largest faults in the volume.

We want to be able to sum the contributions from many faults, none of which in general, has dimensions comparable to the dimensions of the volume over which we are averaging. Thus the dimensions of the fault areas $A^{(i)}$ and the dimensions of the volume $\mathcal{V}$ do not, in general, cancel out. If, however, we analyze a situation in which one or more faults cut completely through the volume $\mathcal{V}$, then the fault area, projected onto a plane normal to $\mathbf{t}$ and within $\mathcal{V}$, is identical to the cross-sectional area of $\mathcal{V}$ as measured on the plane normal to $\mathbf{t}$. Therefore the numerator and denominator of Eq. (2.1.10) are equal, and the probability is exactly 1 that a random line parallel to $\mathbf{t}$ through the volume will intersect the fault (see Fig. 2A and Eq. (2.3.5) for an example).

We can write the fault area $A^{(i)}$ in Eq. (2.1.12) in terms of the horizontal length $L^{(i)}$ of the fault, as follows:

$$A^{(i)} = \left(\lambda^{(i)}L^{(i)}\right)L^{(i)} = \lambda^{(i)}\left(L^{(i)}\right)^2, \quad \lambda^{(i)} \equiv \frac{A^{(i)}}{\left(L^{(i)}\right)^2}, \tag{2.1.13}$$

where $\lambda^{(i)}$ is a geometrical constant that accounts for the difference between the horizontal length and down-dip width of the fault as well as for the shape of the fault. For example, if the fault is rectangular in shape with horizontal length $L^{(i)}$ and down-dip width $l^{(i)}$, or if it is elliptical in shape with a horizontal major-axis length $L^{(i)}$ and a down-dip minor-axis length $l^{(i)}$ then, respectively,

$$\lambda^{(i)} = 1\frac{l^{(i)}}{L^{(i)}} \quad \text{or} \quad \lambda^{(i)} = \frac{\pi}{4}\frac{l^{(i)}}{L^{(i)}}. \tag{2.1.14}$$

If we wish to average the effects of multiple faults in a volume, the dimensions of the volume $\mathcal{V}$ over which we are averaging (Eq. (2.1.8)) must be large relative to the dimensions of the largest fault, although the actual depth to which the volume extends is limited by the thickness of the brittle crust. In Section 3 we will be able to be more specific about what 'large' means in this context (see Eqs. (3.4.2)–(3.4.4) and Part II, Section 3).

Substituting Eqs. $(2.1.13)_1$ into Eqs. (2.1.6) and (2.1.10) gives,

$$\left.\begin{aligned} e^{(i)}_{(3,t)} &= \frac{\lambda^{(i)}\left(L^{(i)}\right)^2}{\mathcal{V}}\cos\theta^{(i)}\delta^{(i)}\cos\phi^{(i)}, \\ {}_3\mathfrak{P}^{(i)}_t &= \frac{\lambda^{(i)}\left(L^{(i)}\right)^2\cos\theta^{(i)}}{\mathcal{A}_t}, \\ e^{(i)}_{(3,t)} &= {}_3\mathfrak{P}^{(i)}_t\frac{\delta^{(i)}\cos\phi^{(i)}}{\mathcal{T}}. \end{aligned}\right\} \tag{2.1.15}$$

We pursue this analysis for a simple case, for which we assume all the faults, regardless of size, have a similar shape and orientation, so the geometrical factor λ and fault-orientation angle θ are the same for all faults; all the displacements have a similar orientation, so the angle ϕ is the same for all of the faults; and the fault population is homogeneously distributed throughout the volume. Faults with conjugate orientations easily can be included in the analysis (see for example Section 2.3, Eq. (2.3.5)), but for simplicity we consider only faults having the same orientation. For the convenience of future reference to one equation, we include in this definition of the simple case, angles $\alpha^{(i)}$, $\beta^{(i)}$, $\rho^{(i)}$, $\kappa^{(i)}$, and $\varepsilon^{(i)}$ (see Fig. 1 and Eqs. (2.2.2), (3.1.20), and (S2.1.8)), and geometric parameters $\mu^{(i)}$ and $\nu^{(i)}$ that are defined later in the paper (see Eqs. (3.1.21) and (4.1.10)).

$$\begin{aligned} &\text{For all } i: \\ &\theta^{(i)} = \theta, \quad \phi^{(i)} = \phi, \quad \alpha^{(i)} = \alpha, \quad \beta^{(i)} = \beta, \\ &\rho^{(i)} = \rho, \quad \kappa^{(i)} = \kappa, \quad \varepsilon^{(i)} = \varepsilon, \\ &\lambda^{(i)} = \lambda, \quad \mu^{(i)} = \mu, \quad \nu^{(i)} = \nu. \end{aligned} \tag{2.1.16}$$

With these simplifications, the contribution of the ith fault to the total extension of the volume $\mathcal{V}$ parallel to $\mathbf{t}$ can be written from Eq. $(2.1.15)_1$

$$e^{(i)}_{(3,t)} = \frac{\lambda\left(L^{(i)}\right)^2}{\mathcal{V}}\delta^{(i)}\cos\theta\cos\phi, \tag{2.1.17}$$

and the total volume-averaged continuum extension parallel to $\mathbf{t}$, following Eq. (2.1.12), is therefore the sum of the weighted local extensions (Eq. (2.1.17)) from all the faults in the volume,

$$e^{(\mathrm{tot})}_{(3,t)} = \sum_{i=1}^{N^{(\max)}} e^{(i)}_{(3,t)} = \frac{\lambda\cos\theta\cos\phi}{\mathcal{V}}\sum_{i=1}^{N^{(\max)}}\left(L^{(i)}\right)^2\delta^{(i)}. \tag{2.1.18}$$

2.2. Infinitesimal continuum shear strain from brittle faulting

The second problem we address is how to find the continuum shear strain from a distributed brittle deformation. We apply an analysis similar to that used in the preceding section (Section 2.1). The continuum tensor shear strain of a line parallel to the unit vector **t**, relative to an initially orthogonal line parallel to the unit vector **w** (Fig. 1), is obtained from the strain tensor by

$$e_{(3,\gamma)} = e_{kl}t_k w_l, \tag{2.2.1}$$

where the subscript '3' identifies the strain as applying to the three-dimensional volume $\mathcal{V}$, and the subscript γ indicates the strain is the shear strain of a pair of initially orthogonal material lines parallel to **t** and **w**. We define α to be the angle between the normal to the fault plane, **n**, and the direction **w**, and β to be the angle between the fault-slip direction **η** and the direction **w** (Fig. 1A), whereby,

$$n_l w_l = \cos\alpha, \quad \eta_l w_l = \cos\beta. \tag{2.2.2}$$

Substituting for the strain tensor in Eq. (2.2.1) from Eq. (2.1.1) with (2.1.2), and using Eqs. (2.2.2), gives for the ith fault in a set of $N^{(\max)}$ faults (see Fig. 2),

$$e^{(i)}_{(3,\gamma)} = \frac{A^{(i)}\delta^{(i)}}{\mathcal{V}}\frac{1}{2}\left[\cos\phi^{(i)}\cos\alpha^{(i)} + \cos\theta^{(i)}\cos\beta^{(i)}\right], \tag{2.2.3}$$

Using Eq. (2.1.8), we can rewrite Eq. (2.2.3) as

$$e^{(i)}_{(3,\gamma)} = \frac{1}{2}\left\{\left[\frac{A^{(i)}\cos\theta^{(i)}}{(\mathcal{V}/\mathcal{T})}\right]\left[\frac{\delta^{(i)}\cos\beta^{(i)}}{\mathcal{T}}\right] + \left[\frac{A^{(i)}\cos\alpha^{(i)}}{(\mathcal{V}/\mathcal{W})}\right] \times \left[\frac{\delta^{(i)}\cos\phi^{(i)}}{\mathcal{W}}\right]\right\}. \tag{2.2.4}$$

Within the braces {…} is the sum of two terms, each with two factors. In the first term, the first factor in brackets […] is a weighting that is the probability that a random line through the volume $\mathcal{V}$ parallel to **t** intersects the ith fault (Eq. (2.1.10)); and the second factor in brackets is the local shear strain of the line $\mathcal{T}$ due to the component of slip on the fault in the direction **w** perpendicular to **t**. The second term is similar, except the first factor is the probability that a random line parallel to **w** through the volume $\mathcal{V}$ intersects the ith fault,

$${}_3\mathfrak{P}^{(i)}_w = \frac{A^{(i)}\cos\alpha^{(i)}}{(\mathcal{V}/\mathcal{W})} = \frac{A^{(i)}\cos\alpha^{(i)}}{\mathcal{A}_w}, \tag{2.2.5}$$

and the second factor is the local shear strain of the line $\mathcal{W}$ due to the component of slip on the fault in the direction **t** perpendicular to **w**. Thus, substituting Eqs. (2.1.10) and (2.2.5) into (2.2.4) gives:

$$e^{(i)}_{(3,\gamma)} = \frac{1}{2}\left\{{}_3\mathfrak{P}^{(i)}_t\left[\frac{\delta^{(i)}\cos\beta^{(i)}}{\mathcal{T}}\right] + {}_3\mathfrak{P}^{(i)}_w\left[\frac{\delta^{(i)}\cos\phi^{(i)}}{\mathcal{W}}\right]\right\}. \tag{2.2.6}$$

This equation says that half the sum of these shear terms is the symmetric continuum shear strain for material lines parallel to **t** relative to material lines parallel to **w**. If the fault plane is parallel to **w**, then $\alpha = 90^\circ$, ${}_3\mathfrak{P}^{(i)}_w = 0$, and the second term is zero.

We use Eq. $(2.1.13)_2$ in Eq. (2.2.3), and sum the result over all $N^{(\max)}$ faults in the volume $\mathcal{V}$ to find the total tensor shear strain of the volume,

$$e^{(\mathrm{tot})}_{(3,\gamma)} = \sum_{i=1}^{N^{(\max)}} e^{(i)}_{(3,\gamma)} = \sum_{i=1}^{N^{(\max)}} \frac{\lambda^{(i)}\left(L^{(i)}\right)^2\delta^{(i)}}{2\mathcal{V}}\left[\cos\theta^{(i)}\cos\beta^{(i)} + \cos\phi^{(i)}\cos\alpha^{(i)}\right]. \tag{2.2.7}$$

As in Eq. (2.1.12), we assume the faults are numbered $i = 1{:}N^{(\max)}$ in order of decreasing displacement magnitude. Thus a partial sum over $N < N^{(\max)}$ faults gives the cumulative contribution to the shear strain of the N faults that have the largest displacements in the volume.

For our analysis of a simple special case, we assume the conditions in Eq. (2.1.16), which require that all faults have the same shape and orientation, and that the slip directions all have the same orientation. These assumptions, with Equation $(2.1.13)_2$, simplify Eq. (2.2.3) to

$$e^{(i)}_{(3,\gamma)} = \frac{\lambda\left(L^{(i)}\right)^2\delta^{(i)}}{\mathcal{V}}\frac{1}{2}[\cos\theta\cos\beta + \cos\phi\cos\alpha]. \tag{2.2.8}$$

The expression for the total tensor shear strain of the volume $\mathcal{V}$ (Eq. (2.2.7)) becomes

$$e^{(\mathrm{tot})}_{(3,\gamma)} = \sum_{i=1}^{N^{(\max)}} e^{(i)}_{(3,\gamma)} = \frac{\lambda}{2\mathcal{V}}[\cos\theta\cos\beta + \cos\phi\cos\alpha]\sum_{i=1}^{N^{(\max)}}\left(L^{(i)}\right)^2\delta^{(i)}. \tag{2.2.9}$$

2.3. Simple example of extensional strain

We can apply Eq. (2.1.12) to a simple example comparable to that used by Peacock and Sanderson (1993). Fig. 2A shows a block cut by two conjugate normal faults, each dipping at 60° with down-dip displacement of $\delta = 1$ m. From inspection, the extension of a horizontal line parallel to the front face of the block is

$$e^{(\mathrm{tot})}_{(3,t)} = \sum_{i=1}^{2}\frac{\Delta\mathcal{T}^{(i)}_t}{\mathcal{T}_0} = \frac{0.5}{100} + \frac{0.5}{100} = 0.01. \tag{2.3.1}$$

For comparison with Eq. (2.3.1), we apply Eq. (2.1.12) to the calculation. The area of the ith fault plane is the down-dip width of the plane times the length parallel to strike. For this example, therefore, we have from Fig. 2A,

$$A^{(i)} = \frac{\mathcal{H}_0}{|\cos\theta^{(i)}|}\mathcal{W}_0, \quad \mathcal{V} = \mathcal{T}_0\mathcal{W}_0\mathcal{H}_0, \tag{2.3.2}$$

$$\mathcal{T}_0 \approx \mathcal{T} = 100\ \mathrm{m}, \quad \delta^{(i)} = 1\ \mathrm{m}, \tag{2.3.3}$$

$$\begin{aligned}\theta^{(1)} &= \angle\left(\mathbf{n}^{(1)},\mathbf{t}\right) = 30^\circ,\ \theta^{(2)} = \angle\left(\mathbf{n}^{(2)},\mathbf{t}\right) = 150^\circ,\\ \phi^{(1)} &= \angle\left(\boldsymbol{\delta}^{(1)},\mathbf{t}\right) = 60^\circ,\ \phi^{(2)} = \angle\left(\boldsymbol{\delta}^{(2)},\mathbf{t}\right) = 120^\circ,\end{aligned} \tag{2.3.4}$$

where Eq. $(2.3.3)_1$ is the infinitesimal strain approximation from Eq. $(2.1.11)_1$, and the displacement vector $\boldsymbol{\delta}^{(i)}$ is defined in Eq. $(2.1.3)_2$. Eq. (2.1.12) with Eqs. (2.3.2) then gives,

$$e^{(\mathrm{tot})}_{(3,t)} = \sum_{i=1}^{2}\mathrm{sgn}\left(\cos\theta^{(i)}\right)\frac{\delta^{(i)}\cos\phi^{(i)}}{\mathcal{T}},\ \mathrm{sgn}\left(\cos\theta^{(i)}\right) \equiv \frac{\cos\theta^{(i)}}{|\cos\theta^{(i)}|} = \pm 1. \tag{2.3.5}$$

The function $\mathrm{sgn}(\cos\theta^{(i)})$ accounts for the conjugate orientations of the faults in this example (Fig. 2A; Eq. (2.3.4)). In this case, the weighting term in Eq. (2.1.7), which is defined as ${}_3\mathfrak{P}^{(i)}_t$ in Eq. (2.1.10), is equal to 1, which is consistent with our discussion above, because the faults in this example cut completely through the volume (Fig. 2A). Eq. $(2.3.5)_1$ then gives,

$$e^{(\mathrm{tot})}_{(3,t)} = (+1)\frac{(1)\cos 60^\circ}{100} + (-1)\frac{(1)\cos 120^\circ}{100} = \frac{(0.5)}{100} + \frac{(0.5)}{100} = 0.01. \tag{2.3.6}$$

Thus Eq. (2.1.12) gives the anticipated answer for this simple example.

2.4. Simple example of shear strain

We apply the equations for the shear strain in a volume, to the simple example in Fig. 2B, where the slip on each of the two faults is assumed to be $\delta = 1$ m, and the dimensions of each fault block are 100 m by 50 m. From inspection, we can see that the tensor shear strain averaged over the shear zone is,

$$e^{(\mathrm{tot})}_{(3,\gamma)} = \frac{1}{2}\sum_{i=1}^{2}\frac{\delta^{(i)}}{\mathcal{T}_0} = \frac{1}{2}\left(\frac{1}{100}+\frac{1}{100}\right) = 0.01, \tag{2.4.1}$$

and the shear angle ψ is given by,

$$\psi = \tan^{-1}\frac{2}{100} = 1.15^\circ = 0.02 \text{ rad}. \tag{2.4.2}$$

For comparison with this calculation, we apply Eq. (2.2.7). Assuming the thickness of the blocks normal to the diagram is $\mathcal{H}_0$ m, we have

$$\left.\begin{aligned} L^{(i)} &= \mathcal{W}_0, \quad \lambda^{(i)} = \mathcal{H}_0/\mathcal{W}_0, \\ A^{(i)}_t &= \mathcal{W}_0\mathcal{H}_0, \quad \mathcal{V}_0 = \mathcal{T}_0\mathcal{W}_0\mathcal{H}_0, \end{aligned}\right\} \tag{2.4.3}$$

$$\mathcal{T}_0 = 100\text{ m}, \quad \mathcal{W}_0 = 100\text{ m}, \quad \delta^{(i)} = 1\text{ m}, \tag{2.4.4}$$

$$\left.\begin{aligned} \theta^{(i)} &= \angle\left(\mathbf{n}^{(i)},\mathbf{t}\right) = 0^\circ,\ \alpha^{(i)} = \angle\left(\mathbf{n}^{(i)},\mathbf{w}\right) = 90^\circ, \\ \phi^{(i)} &= \angle\left(\boldsymbol{\eta}^{(i)},\mathbf{t}\right) = 90^\circ,\ \beta^{(i)} = \angle\left(\boldsymbol{\eta}^{(i)},\mathbf{w}\right) = 0^\circ, \end{aligned}\right\} \tag{2.4.5}$$

whereby Eq. (2.2.7) gives

$$e^{(\mathrm{tot})}_{(3,\gamma)} = \frac{1}{2\cdot 100}[2(\cos 0^\circ\cos 0^\circ + \cos 90^\circ\cos 90^\circ)] = 0.01. \tag{2.4.6}$$

Thus the shear strain given by Eq. (2.2.7) gives the result anticipated from the direct calculation from Fig. 2B. Eq. (2.1.10) with Eq. (2.1.11) and the values given in Eqs. (2.4.3)–(2.4.5) show that the probability ${}_3\mathfrak{P}^{(i)}_t$ is 1 that a horizontal sampling line normal to the strike of the faults cuts both faults, as required by the fact that the faults both cut through the entire volume. For the geometry of this example, the probability ${}_3\mathfrak{P}^{(i)}_w$ is zero, as shown by Eq. (2.2.5) with Eqs. (2.4.3)–(2.4.5).

3. Fault population systematics for sampling domains of different dimensionality

3.1. Equations describing fault systematics

Eqs. (2.1.18) or (2.2.9) imply that we need to measure the displacements on all the faults of all sizes within the volume $\mathcal{V}$. Such a measurement, however, is impossible because we can never sample the interior of a volume completely. Even if mine tunnels or drill core is available, they provide only partial sampling of the volume, and seismic profiles are of limited resolution. Moreover, given the usual incomplete exposure in outcrop, the measurement of displacements on all the faults along a linear traverse is in general also impossible. It is not even apparent that we could make a meaningful estimate of the extension by measuring only the largest faults, because although smaller faults have smaller displacements, the number of faults increases rapidly as the size of the faults decreases.

To overcome these problems, we can use the scaling relations for fault-length and fault-displacement to estimate the total extension or shear strain without having to measure all faults. Empirically, the displacement on a fault is related to the length of the fault by a power-law (e.g. Clark and Cox, 1996; Kim and Sanderson, 2005) (see the companion paper Part II, Fig. II:1):

$$L^p = B\delta \quad \text{or} \quad p\log L = \log B + \log\delta, \tag{3.1.1}$$

$$\delta = \frac{1}{B}L^p \quad \text{or} \quad \log\delta = -\log B + p\log L, \tag{3.1.2}$$

where δ represents the mean of the displacement distribution across the area of a fault. The constant $1/B$ defines the displacement on faults that have unit length in any specific area.

Numerous studies (e.g. Cladouhos and Marrett, 1996; Watterson et al., 1996) also have shown a power-law distribution for the cumulative number $N(L)$ or the cumulative frequency $f(L)$ of faults as a function of fault-length. Here, $N(L)$ and $f(L)$ define the cumulative number and frequency, respectively, of faults that have a length greater than or equal to L. The cumulative frequency is defined to be the cumulative number of faults per unit size of the sampling domain. These power-law relations are given by,

$$N_{(\zeta,v)}(L) = G_{(\zeta,v)}L^{-m_\zeta}, \ \log N_{(\zeta,v)}(L) = \log G_{(\zeta,v)} - m_\zeta\log L, \tag{3.1.3}$$

$$f_{(\zeta,v)}(L) = g_{(\zeta,v)}L^{-m_\zeta}, \ \log f_{(\zeta,v)}(L) = \log g_{(\zeta,v)} - m_\zeta\log L. \tag{3.1.4}$$

In these equations, the Greek subscript ζ is used to indicate the dimensionality of the domain in which the sampling of the faults is done, accounting for the fact that different relations are derived from the sampling of faults in the volume ($\zeta = 3$), on a two-dimensional surface ($\zeta = 2$), or along a linear transect ($\zeta = 1$) (although measuring the length of a fault intersected by linear transect implies some access to at least one other dimension). In the subscript '(ζ,v)', the 'v' indicates the orientation of the sampling domain. In this development, 'v' can stand for 't', 'w', or '$\perp h$', indicating respectively linear domains parallel to **t** or to **w**, or planar domains perpendicular to **h**. If $\zeta = 3$, the sampling domain is the entire volume $\mathcal{V}$, and the subscript 'v' is not needed. The constants $G_{(\zeta,v)}$ and $g_{(\zeta,v)}$ are the cumulative number and the cumulative frequency, respectively, of faults having a length greater than or equal to 1, in the prevailing units used for the measurements. Thus these parameters calibrate the fracture intensity, which is specific to individual regions of fracturing, and also to specific orientations of one- and two-dimensional sampling domains.

The cumulative functions and the parameters in the two Eqs. (3.1.3) and (3.1.4) are related respectively by,

$$f_{(\zeta,v)}(L) \equiv N_{(\zeta,v)}(L)/\Delta_{(\zeta,v)}, \quad g_{(\zeta,v)} \equiv G_{(\zeta,v)}/\Delta_{(\zeta,v)}, \tag{3.1.5}$$

where $\Delta_{(\zeta,v)}$ is the size of the ζ-dimensional sampling domain, as defined by (Fig. 2A),

$$\Delta_{(3)} \equiv \mathcal{V} = \mathcal{T}\mathcal{W}\mathcal{H}, \ \Delta_{(2,\perp h)} \equiv \mathcal{A}_h = \mathcal{T}\mathcal{W}, \ \Delta_{(1,v)} \equiv \left\{\begin{array}{l} \mathcal{T} \text{ for } v = t \\ \mathcal{W} \text{ for } v = w \end{array}\right\}, \tag{3.1.6}$$

and where $\mathcal{T}$ (or $\mathcal{W}$) is the length of the horizontal dimension of the volume $\mathcal{V}$ parallel to the unit vector **t** (or **w**), the choice depending on the orientation of the specific line under consideration, and $\mathcal{A}_h$ is a horizontal (map) area normal to the vertical unit vector **h**, which is parallel to the dimension $\mathcal{H}$ of the volume $\mathcal{V}$ (see the companion paper, Part II, Fig. II:2B and II:4B for data sets illustrating, respectively, Eq. $(3.1.4)_2$ and $(3.1.3)_2$, for $\zeta = 2$).

Substituting for L or $\log L$ in Eqs. (3.1.3) and (3.1.4) from the Eq. $(3.1.1)_1$ or $(3.1.1)_2$, respectively, we see that the cumulative number or cumulative frequency of fault-displacements must also have a power-law distribution,

$$N_{(\zeta,\nu)}(\delta) = G_{(\zeta,\nu)}(B\delta)^{-m_\zeta/p},$$
$$\log N_{(\zeta,\nu)}(\delta) = \log\left(G_{(\zeta,\nu)}B^{-m_\zeta/p}\right) - \frac{m_\zeta}{p}\log\delta, \quad (3.1.7)$$

$$f_{(\zeta,\nu)}(\delta) = g_{(\zeta,\nu)}(B\delta)^{-m_\zeta/p},$$
$$\log f_{(\zeta,\nu)}(\delta) = \log\left(g_{(\zeta,\nu)}B^{-m_\zeta/p}\right) - \frac{m_\zeta}{p}\log\delta, \quad (3.1.8)$$

$N_{(\zeta,\nu)}(\delta)$ and $f_{(\zeta,\nu)}(\delta)$ are respectively the cumulative number and the cumulative frequency of faults that have a displacement greater than or equal to δ in the sampling of a ζ-dimensional domain, the orientation of which is defined by ν.

We introduce the parameters s_ζ, $R_{(\zeta,\nu)}$, and $r_{(\zeta,\nu)}$ by the definitions,

$$s_\zeta \equiv \frac{m_\zeta}{p}, \quad R_{(\zeta,\nu)} \equiv G_{(\zeta,\nu)}B^{-s_\zeta} = G_{(\zeta,\nu)}B^{-m_\zeta/p},$$
$$r_{(\zeta,\nu)} \equiv g_{(\zeta,\nu)}B^{-s_\zeta} = g_{(\zeta,\nu)}B^{-m_\zeta/p}, \quad (3.1.9)$$

whereby Eqs. (3.1.7) and (3.1.8) become

$$N_{(\zeta,\nu)}(\delta) = R_{(\zeta,\nu)}\delta^{-s_\zeta}, \ \log N_{(\zeta,\nu)}(\delta) = \log R_{(\zeta,\nu)} - s_\zeta\log\delta, \quad (3.1.10)$$

$$f_{(\zeta,\nu)}(\delta) = r_{(\zeta,\nu)}\delta^{-s_\zeta}, \ \log f_{(\zeta,\nu)}(\delta) = \log r_{(\zeta,\nu)} - s_\zeta\log\delta. \quad (3.1.11)$$

Here, the constants $R_{(\zeta,\nu)}$ and $r_{(\zeta,\nu)}$ are the cumulative number and cumulative frequency, respectively, for faults on which the displacement is greater than or equal to 1, in the prevailing units, in a ζ-dimensional sampling domain that has an orientation defined by ν (see Fig. 3A and the companion paper, Part II, Fig. II:4D, for data illustrating Eq. $(3.1.10)_2$ for $\zeta = 1$ and 2, respectively; see Fig. 3B, and II:4C for data illustrating Eq. $(3.1.11)_2$ for $\zeta = 1$). From Eqs. $(3.1.9)_2$, $(3.1.9)_3$, and $(3.1.5)_2$, we have the relation

$$r_{(\zeta,\nu)} = R_{(\zeta,\nu)}/\Delta_{(\zeta,\nu)}. \quad (3.1.12)$$

From Eqs. $(3.1.10)_1$, $(3.1.11)_1$, and (3.1.12), we see that

$$f_{(\zeta,\nu)}(\delta) = \frac{N_{(\zeta,\nu)}(\delta)}{\Delta_{(\zeta,\nu)}}. \quad (3.1.13)$$

Clearly, the total number of faults $R_{(\zeta,\nu)}$ having a displacement greater than or equal to 1 must change as the size of the sampling domain changes, and thus it is not a characteristic of the fault population from a given region. On the other hand, the frequency of such faults $r_{(\zeta,\nu)}$ is independent of the size of the domain, as the number of faults having a displacement greater than or equal to 1 is normalized by the size of the sampling domain (Eq. (3.1.12)) (see Fig. 3A and B for plots of the same data using cumulative number and cumulative frequency with $\zeta = 1$). Thus formulating the equations for the systematics of both length (Eqs. (3.1.4)) and displacement (Eqs. (3.1.11)) in terms of the frequency eliminates the non-uniqueness associated with the finite size of the sampling domain and results in a single equation that characterizes similar fault populations in all domains of the same dimensionality in a homogeneously faulted region. It thus provides the preferred method for comparing results for different-sized domains. It is easy to switch between the cumulative number and the cumulative frequency relations, as convenience dictates, using either Eqs. (3.1.5) or Eq. (3.1.13) with Eq. (3.1.12), and applying the definitions in Eq. (3.1.6). Note, however, that for $\zeta = 1$ or 2, both $R_{(\zeta,\nu)}$ and $r_{(\zeta,\nu)}$ can change with the orientation ν of the sampling domain if the faults have a preferred orientation, as is usually the case.

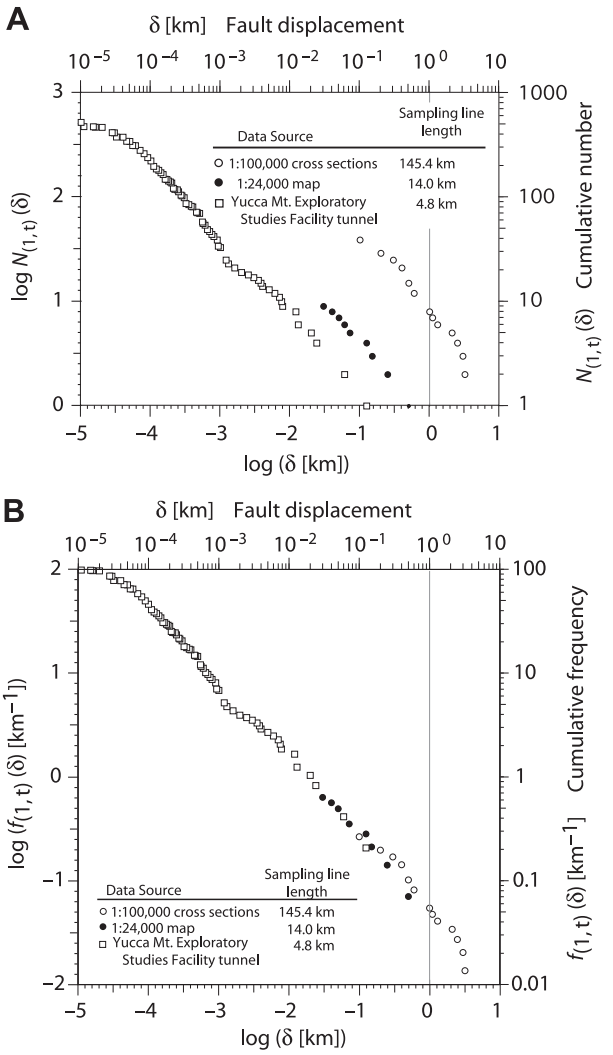

Fig. 3. Fault-displacement systematics measured from one-dimensional sampling in the Paintbrush tuff, Yucca Mountain, Nevada. Sample line lengths for the different data sets, which have been sampled at different scales, are listed in the insets on the graphs (from Marrett et al., 1999). The two plots illustrate the difference between plotting the displacement against cumulative number and cumulative frequency. A. Data plotted as logarithm of displacement [km] vs. the logarithm of cumulative number. B. Same data as in Part A plotted as the logarithm of displacement [km] vs. logarithm of cumulative frequency. Solid line is the best fit to the linear part of the data.

The frequency of faults having a length between L and $L + \mathrm{d}L$, or a displacement between δ and $\delta + \mathrm{d}\delta$, is just the differential of the cumulative frequency distribution $f_{(\zeta,\nu)}$ measured in a ζ-dimensional sampling domain that has an orientation given by ν. Taking the differential of Eqs. $(3.1.4)_1$ and $(3.1.11)_1$, we find, respectively,

$$\mathrm{d}f_{(\zeta,\nu)}(L) = -m_\zeta g_{(\zeta,\nu)}L^{(-m_\zeta-1)}\,\mathrm{d}L, \ \mathrm{d}f_{(\zeta,\nu)}(\delta) = -s_\zeta r_{(\zeta,\nu)}\delta^{(-s_\zeta-1)}\,\mathrm{d}\delta. \quad (3.1.14)$$

The actual number of faults in each increment is obtained from the differential frequency equations simply by multiplying the differential frequency $\mathrm{d}f_{(\zeta,\nu)}$ by the size of the domain $\Delta_{(\zeta,\nu)}$, as defined in Eq. (3.1.6).

Before using these scaling relationships to estimate the sums in Eqs. (2.1.18) and (2.2.9), we must clarify the effect of the dimensionality of the sampling domain on the constants in these

equations. Ideally, we would like to determine the strain in a volume $\mathcal{V}$ that results from displacement on a set of distributed faults by doing a complete three-dimensional sampling of the faults within that volume ($\zeta = 3$). As discussed at the beginning of Section 3.1, such a sampling is impossible in practice, so in general, the scaling relations must be determined from measurements made on two-dimensional surfaces ($\zeta = 2$) or along one-dimensional lines ($\zeta = 1$). Thus we need to find how the scaling relations for one- and two-dimensional sampling are related to the relations for three-dimensional sampling.

To this end, we write the relations between the incremental numbers of faults as,

$$\mathrm{d}N_{(1,t)} = {}_3\mathfrak{P}_t\,\mathrm{d}N_{(3)},\ \mathrm{d}N_{(1,w)} = {}_3\mathfrak{P}_w\,\mathrm{d}N_{(3)},\ \mathrm{d}N_{(2,\perp h)} = {}_3\mathfrak{P}_{\perp h}\,\mathrm{d}N_{(3)}, \tag{3.1.15}$$

where for the subscripts in parentheses on the cumulative number N, the numeric subscript indicates the dimensionality of the sampling domain, and the letter subscript (not used for a three-dimensional domain) indicates the orientation of the sampling domain, which is either a line parallel to the unit vector **t** or **w**, or a plane perpendicular to the unit vector **h**. ${}_3\mathfrak{P}_t$, ${}_3\mathfrak{P}_w$, and ${}_3\mathfrak{P}_{\perp h}$ are the probabilities that a fault of a given length or displacement in a three-dimensional domain (the volume $\mathcal{V}$; left subscript) will be intersected, respectively, by a randomly located line parallel to **t** or **w** through the volume, or by a randomly located plane perpendicular to **h** through the volume (right subscript). These probabilities are expressed as continuous functions of either fault-length or fault-displacement. The incremental number of faults along the direction **w** differs from that along the direction **t** only because of the difference in orientation of the line, so at this point we develop the relations only for **t.** In terms of the frequencies, we use Eqs. (3.1.5) and (3.1.6) to write Eqs. (3.1.15) as,

$$\mathrm{d}f_{(1,t)}(L) = {}_3\mathfrak{p}_t\,\mathrm{d}f_{(3)}(L),\quad \mathrm{d}f_{(1,t)}(\delta) = {}_3\mathfrak{p}_t\,\mathrm{d}f_{(3)}(\delta), \tag{3.1.16}$$

$$\mathrm{d}f_{(2,\perp h)}(L) = {}_3\mathfrak{p}_{\perp h}\,\mathrm{d}f_{(3)}(L),\quad \mathrm{d}f_{(2,\perp h)}(\delta) = {}_3\mathfrak{p}_{\perp h}\,\mathrm{d}f_{(3)}(\delta), \tag{3.1.17}$$

where

$${}_3\mathfrak{p}_t \equiv \frac{\mathcal{V}}{\mathcal{T}}\,{}_3\mathfrak{P}_t,\quad {}_3\mathfrak{p}_{\perp h} \equiv \frac{\mathcal{V}}{\mathcal{A}_h}\,{}_3\mathfrak{P}_{\perp h}. \tag{3.1.18}$$

Thus Eqs. $(3.1.16)_1$ with $(3.1.18)_1$ state that the differential $\mathrm{d}f_{(1,t)}(L)$ is the frequency with which faults having lengths between L and $L + \mathrm{d}L$ are intersected by a sampling line parallel to **t** through the portion of the volume $\mathcal{V}$ that is associated with a unit length of the sampling line. Eq. $(3.1.16)_2$ with $(3.1.18)_1$ has a comparable meaning with respect to the displacement δ, and we could write similar equations for a sampling line parallel to **w** by substituting '*w*' for '*t*' in Eqs. (3.1.16) and $(3.1.18)_1$. Eqs. (3.1.17) with $(3.1.18)_2$ have comparable meanings with respect to the two-dimensional sampling domain normal to **h**.

We now obtain relations for the probabilities ${}_3\mathfrak{P}_t$, ${}_3\mathfrak{P}_{\perp h}$, ${}_3\mathfrak{p}_t$, and ${}_3\mathfrak{p}_{\perp h}$ in terms of the fault-length and fault-displacement. The probability ${}_3\mathfrak{P}_t^{(i)}$ that the ith fault in a volume $\mathcal{V}$ will intersected by a randomly located line across $\mathcal{V}$ parallel to the unit vector **t**, is just the area of the fault projected normal to **t**, divided by the cross-sectional area $\mathcal{A}_t$ of the volume $\mathcal{V}$ normal to **t**. Introducing Eq. $(3.1.1)_1$ for the ith fault into Eq. $(2.1.15)_2$ gives,

$${}_3\mathfrak{P}_t^{(i)} = \frac{\lambda^{(i)} B^{2/p}\left(\delta^{(i)}\right)^{2/p}\cos\theta^{(i)}}{\mathcal{A}_t}. \tag{3.1.19}$$

Similarly, the probability ${}_3\mathfrak{P}_{\perp h}^{(i)}$ that the ith fault in a volume $\mathcal{V}$ will be intersected by a randomly located horizontal plane across $\mathcal{V}$ normal to the unit vector **h** (Fig. 1B) is just the vertical component of the down-dip width of the fault divided by the vertical dimension $\mathcal{H}$ of the volume,

$${}_3\mathfrak{P}_{\perp h}^{(i)} = \frac{\mu^{(i)} L^{(i)}\sin\rho^{(i)}}{\mathcal{H}} = \frac{\mu^{(i)} B^{1/p}\left(\delta^{(i)}\right)^{1/p}\sin\rho^{(i)}}{\mathcal{H}}, \tag{3.1.20}$$

where $\rho^{(i)}$ is the fault dip, and the down-dip width of the fault $l^{(i)}$ is

$$l^{(i)} = \mu^{(i)} L^{(i)},\quad \mu^{(i)} \equiv \frac{l^{(i)}}{L^{(i)}}. \tag{3.1.21}$$

Note that $\mu^{(i)} = \lambda^{(i)}$ only for a rectangular-shaped fault (see Eq. $(2.1.14)_1$).

If we make the simplifying assumptions that all faults have the same shape and orientation (Eq. (2.1.16)), then λ, μ, α, θ, and ρ are all constants, and the probabilities are,

$$\left.\begin{aligned} {}_3\mathfrak{P}_t^{(i)} &= \frac{\lambda\left(L^{(i)}\right)^2\cos\theta}{\mathcal{A}_t} = \frac{\lambda B^{2/p}\left(\delta^{(i)}\right)^{2/p}\cos\theta}{\mathcal{A}_t}, \\ {}_3\mathfrak{P}_{\perp h}^{(i)} &= \frac{\mu L^{(i)}\sin\rho}{\mathcal{H}} = \frac{\mu B^{1/p}\left(\delta^{(i)}\right)^{1/p}\sin\rho}{\mathcal{H}}. \end{aligned}\right\} \tag{3.1.22}$$

We can then express the probabilities for the individual faults, Eqs. (3.1.22), in terms of a continuous function of fault-length L or fault-displacement δ by,

$${}_3\mathfrak{P}_t = \frac{\lambda\cos\theta}{\mathcal{A}_t}L^2 = \frac{\lambda B^{2/p}\cos\theta}{\mathcal{A}_t}\delta^{2/p}, \tag{3.1.23}$$

$${}_3\mathfrak{P}_{\perp h} = \frac{\mu\sin\rho}{\mathcal{H}}L = \frac{\mu B^{1/p}\sin\rho}{\mathcal{H}}\delta^{1/p}. \tag{3.1.24}$$

From Eq. (3.1.18), the corresponding parameters in Eqs. (3.1.16) and (3.1.17) are

$${}_3\mathfrak{p}_t = \lambda\cos\theta\,L^2 = \lambda B^{2/p}\cos\theta\,\delta^{2/p}, \tag{3.1.25}$$

$${}_3\mathfrak{p}_{\perp h} = \mu\sin\rho\,L = \mu B^{1/p}\sin\rho\,\delta^{1/p}. \tag{3.1.26}$$

Substituting Eqs. (3.1.25) and (3.1.26) respectively into Eqs. (3.1.16) and (3.1.17) gives,

$$\begin{aligned} \mathrm{d}f_{(1,t)}(L) &= \lambda\cos\theta L^2\,\mathrm{d}f_{(3)}(L), \\ \mathrm{d}f_{(1,t)}(\delta) &= \lambda B^{2/p}\cos\theta\,\delta^{2/p}\,\mathrm{d}f_{(3)}(\delta), \end{aligned} \tag{3.1.27}$$

$$\begin{aligned} \mathrm{d}f_{(2,\perp h)}(L) &= \mu\sin\rho L\,\mathrm{d}f_{(3)}(L), \\ \mathrm{d}f_{(2,\perp h)}(\delta) &= \mu B^{1/p}\sin\rho\,\delta^{1/p}\,\mathrm{d}f_{(3)}(\delta). \end{aligned} \tag{3.1.28}$$

Comparable probabilities for lines parallel to **w** can be obtained from Eqs. $(3.1.22)_{1,2}$, (3.1.23), and (3.1.25) by substituting '*w*' for '*t*' and 'α' for 'θ' (see the Supplementary Material, Eq. (S1.1.3)).

$$\left.\begin{aligned} {}_3\mathfrak{P}_w^{(i)} &= \frac{\lambda\left(L^{(i)}\right)^2\cos\alpha}{\mathcal{A}_w} = \frac{\lambda B^{2/p}\left(\delta^{(i)}\right)^{2/p}\cos\alpha}{\mathcal{A}_w}, \\ {}_3\mathfrak{P}_w &= \frac{\lambda\cos\alpha}{\mathcal{A}_w}L^2 = \frac{\lambda B^{2/p}\cos\alpha}{\mathcal{A}_w}\delta^{2/p}, \end{aligned}\right\} \tag{3.1.29}$$

$${}_3\mathfrak{p}_w = \lambda\cos\alpha\,L^2 = \lambda B^{2/p}\cos\alpha\,\delta^{2/p}. \tag{3.1.30}$$

3.2. Relations among parameters in the equations describing fault systematics in domains of different dimensionality

The cumulative number and frequency of faults in a given sampling domain can be described as a function of either fault-length or fault-displacement (Eqs. (3.1.3), (3.1.4), (3.1.10), (3.1.11)). Eqs. (3.1.9) define how the parameters in those two types of equations are related. We now want to find the relations among the parameters that define the cumulative frequency distributions determined from sampling domains of different dimensionality. To that end, we substitute for each of the $df_{(\zeta,v)}$ in Eqs. (3.1.27) and (3.1.28) using the appropriate Eqs. $(3.1.14)_1$ or $(3.1.14)_2$, according to whether we want an expression in terms of L or δ, and using the different values of ζ and (ζ,v) as required by the opposite sides of each of Eq. (3.1.27) or (3.1.28). For example, to find the relations among m_1, m_3, $g_{(1,t)}$, and $g_{(3)}$, we use Eq. $(3.1.14)_1$ first with $\zeta=1$ and $(\zeta,v)=(1,t)$ to substitute for the left of Eq. $(3.1.27)_1$ and then with $\zeta=3$ and $(\zeta,v)=(3)$ to substitute for the right side, to find,

$$-m_1 g_{(1,t)}\, L^{(-m_1-1)} \;=\; -\lambda\cos\theta\; m_3\; g_{(3)}\; L^{(-m_3+1)}. \tag{3.2.1}$$

For this equation to hold for any value of L, the exponents on the L on each side of the equation must be equal, and the coefficients of L on each side of the equation also must be equal. These conditions then give, respectively,

$$m_1 \;=\; m_3-2, \tag{3.2.2}$$

$$g_{(1,t)} \;=\; g_{(3)}\lambda\cos\theta\,\frac{m_3}{(m_3-2)}, \tag{3.2.3}$$

where we also used Eq. (3.2.2) to get Eq. (3.2.3).

By parallel analyses, we obtain the relations among m_2, m_3, $g_{(2,\perp h)}$, and $g_{(3)}$, from Eq. $(3.1.14)_1$ with $\zeta=2$ and $(\zeta,v)=(2,\perp h)$ for the left side of Eq. $(3.1.28)_2$, and with $\zeta=3$ and $(\zeta,v)=(3)$ for the right side; we obtain the relations among s_1, s_3, $r_{(1,t)}$, and $r_{(3)}$ from Eqs. $(3.1.27)_2$ by using $(3.1.14)_2$ with $\zeta=1$ and $(\zeta,v)=(1,t)$ for the left side of Eq. $(3.1.27)_2$ and with $\zeta=3$ and $(\zeta,v)=(3)$ for the right side; and we obtain the relations among s_2, s_3, $r_{(2,\perp h)}$, and $r_{(3)}$ from Eqs. $(3.1.28)_2$ using $(3.1.14)_2$ with $\zeta=2$ and $(\zeta,v)=(2,\perp h)$ for the left side of Eq. $(3.1.28)_2$ and with $\zeta=3$ and $(\zeta,v)=(3)$ for the right side. The results are

$$m_2 \;=\; m_3-1, \tag{3.2.4}$$

$$g_{(2,\perp h)} \;=\; g_{(3)}\mu\sin\rho\,\frac{m_3}{m_3-1}, \tag{3.2.5}$$

$$s_1 \;=\; s_3-\frac{2}{p}, \tag{3.2.6}$$

$$r_{(1,t)} \;=\; r_{(3)}\lambda B^{2/p}\cos\theta\,\frac{s_3}{(s_3-2/p)}, \tag{3.2.7}$$

$$s_2 \;=\; s_3-\frac{1}{p}, \tag{3.2.8}$$

$$r_{(2,\perp h)} \;=\; r_{(3)}\mu B^{1/p}\sin\;\rho\,\frac{s_3}{s_3-1/p}. \tag{3.2.9}$$

Finally we can obtain the relations among the s_ζ and m_ζ from Eq. $(3.1.9)_1$, taking ζ to be first 1 and then 2, and using Eqs. (3.2.2) and (3.2.4), to find respectively,

$$s_1=\frac{m_1}{p}=\frac{m_2-1}{p}=\frac{m_3-2}{p},\quad s_2=\frac{m_2}{p}=\frac{m_3-1}{p}, \tag{3.2.10}$$

$$m_3 \;=\; s_1p+2 \;=\; s_2p+1. \tag{3.2.11}$$

We find the relations between $r_{(\zeta,v)}$, and $g_{(\zeta,v)}$ from Eq. (3.2.7) using Eq. $(3.1.9)_5$ with $\zeta=3$ and $(\zeta,v)=(3)$,

$$r_{(1,t)} \;=\; g_{(3)}B^{-(m_3-2)/p}\;\lambda\cos\theta\,\frac{m_3}{(m_3-2)}, \tag{3.2.12}$$

and similarly, we find from Eq. (3.2.9) using Eq. $(3.1.9)_5$ with $\zeta=3$ and $(\zeta,v)=(3)$,

$$r_{(2,\perp h)} \;=\; g_{(3)}\mu B^{-(m_3-1)/p}\;\sin\rho\,\frac{m_3}{m_3-1}. \tag{3.2.13}$$

All the relations for which $(\zeta,v)=(1,t)$ can also be written for $(\zeta,v)=(1,w)$ simply by substituting the subscript 'w' for 't', and the angle 'α' for 'θ'.

3.3. Relations among the maximum displacements in domains of different dimensionality

The fault with the largest displacement ($\delta^{(\max)}_{(3)}$) is the fault for which $N_3=1$, where the subscript '3' indicates the sampling domain is the three-dimensional volume. Using this condition in Eqs. $(3.1.10)_1$ and $(3.1.11)_1$ with $\zeta=3$ and $(\zeta,v)=(3)$ gives,

$$\text{within domain } \mathcal{V}:\quad R_{(3)} \;=\; \left(\delta^{(\max)}_{(3)}\right)^{s_3},\quad r_{(3)} \;=\; \frac{1}{\mathcal{V}}\left(\delta^{(\max)}_{(3)}\right)^{s_3},$$
$$\delta^{(\max)}_{(3)} \;=\; \left(r_{(3)}\mathcal{V}\right)^{1/s_3}, \tag{3.3.1}$$

where Eq. $(3.3.1)_3$ comes from $(3.3.1)_2$. Eq. $(3.3.1)_2$ also can be obtained from Eq. $(3.1.10)_1$ with (3.1.12) and $(3.1.6)_1$, or from Eq. $(3.3.1)_1$ with (3.1.12). Similar relations apply to two and one dimensions, although the fault for which $N_3=1$ is not, in general, the same as the faults for which $N_2=1$ or $N_1=1$, because the probability is less than 1 that the largest fault $N_3=1$ will be intersected by a two- or one-dimensional sampling domain that is randomly located in the volume $\mathcal{V}$. The comparable relations for a map area $\mathcal{A}_h=\mathcal{TW}$ (Eq. $(3.1.6)_2$; see Fig. 2A) from Eqs. $(3.1.10)_1$ and (3.1.12) with $\zeta=2$ and $(\zeta,v)=(2,\perp h)$ are,

$$\text{within domain } \mathcal{A}_h:\; R_{(2,\perp h)}=\left(\delta^{(\max)}_{(2,\perp h)}\right)^{s_2},\; r_{(2,\perp h)}=\frac{1}{\mathcal{A}_h}\left(\delta^{(\max)}_{(2,\perp h)}\right)^{s_2},$$
$$\delta^{(\max)}_{(2,\perp h)}=\left(r_{(2,\perp h)\mathcal{A}_h}\right)^{1/s_2}, \tag{3.3.2}$$

and for sampling in a one-dimensional domain, i.e. along a line of length $\mathcal{T}$ parallel to $\mathbf{t}$ or a line of length $\mathcal{W}$ parallel to $\mathbf{w}$ (Eq. $(3.1.6)_3$; see Fig. 2A), we have from Eqs. $(3.1.10)_1$ and (3.1.12) with $\zeta=1$ and $(\zeta,v)=(1,t)$ or $(1,w)$,

$$\text{within domain } \mathcal{T}:\quad R_{(1,t)} \;=\; \left(\delta^{(\max)}_{(1,t)}\right)^{s_1},\quad r_{(1,t)} \;=\; \frac{1}{\mathcal{T}}\left(\delta^{(\max)}_{(1,t)}\right)^{s_1},$$
$$\delta^{(\max)}_{(1,t)} \;=\; \left(r_{(1,t)}\mathcal{T}\right)^{1/s_1}, \tag{3.3.3}$$

$$\text{within domain } \mathcal{W}:\; R_{(1,w)}=\left(\delta^{(\max)}_{(1,w)}\right)^{s_1},\; r_{(1,w)}=\frac{1}{\mathcal{W}}\left(\delta^{(\max)}_{(1,w)}\right)^{s_1},$$
$$\delta^{(\max)}_{(1,w)}=\left(r_{(1,w)\mathcal{W}}\right)^{1/s_1}. \tag{3.3.4}$$

We can now see how the maximum displacement for sampling from a one-dimensional domain is related to that for sampling a three-dimensional domain by introducing Eqs. $(3.3.1)_2$ and $(3.3.3)_2$ into Eqs. (3.2.7):

$$\left(\delta^{(\max)}_{(1,t)}\right)^{s_1}=\frac{\lambda B^{2/p}\cos\theta}{\mathcal{V}/\mathcal{T}}\,\frac{s_3}{s_1}\left(\delta^{(\max)}_{(3)}\right)^{s_3}. \tag{3.3.5}$$

From Eq. (3.1.22)$_2$, using Eq. (2.1.9)$_1$ and setting $i=1$, we find the relation,

$$\frac{\lambda B^{2/p}\cos\theta}{\mathcal{V}/\mathcal{T}} = \frac{{}_3\mathfrak{P}_t^{(1)}}{\left(\delta_{(3)}^{(\max)}\right)^{2/p}}. \tag{3.3.6}$$

Substituting Eq. (3.3.6) into Eq. (3.3.5), and using Eq. (3.2.6) to change the exponent on $\delta_{(3)}^{(\max)}$ then gives

$$\delta_{(1,t)}^{(\max)} = \left[{}_3\mathfrak{P}_t^{(1)}\frac{s_3}{s_1}\right]^{1/s_1}\delta_{(3)}^{(\max)}. \tag{3.3.7}$$

We know, however, that

$$\delta_{(1,t)}^{(\max)} \le \delta_{(3)}^{(\max)} \quad \text{so} \quad {}_3\mathfrak{P}_t^{(1)}\frac{s_3}{s_1}\le 1 \quad \text{and} \quad {}_3\mathfrak{P}_t^{(1)}\le\frac{s_1}{s_3}. \tag{3.3.8}$$

This means that along a sampling line that is parallel to **t** and is randomly placed in the volume $\mathcal{V}$, the probability ${}_3\mathfrak{P}_t^{(1)}$ that the maximum displacement observed is actually the maximum displacement in the volume is no greater than s_1/s_3.

Similarly, from Eq. (3.2.9) with Eqs. (3.3.1)$_2$, (2.1.9)$_5$, and (3.3.2)$_2$, we have,

$$\left(\delta_{(2,\perp h)}^{(\max)}\right)^{s_2} = \frac{\mu B^{1/p}\sin\rho}{\mathcal{H}}\frac{s_3}{s_3-1/p}\left(\delta_{(3)}^{(\max)}\right)^{s_3}. \tag{3.3.9}$$

Using Eqs. (3.1.22)$_4$ with $i=1$ and (3.2.8) gives,

$$\frac{\mu B^{1/p}\sin\rho}{\mathcal{H}} = \frac{{}_3\mathfrak{P}_{\perp h}^{(1)}}{\left(\delta_{(2,\perp h)}^{(\max)}\right)^{1/p}}, \tag{3.3.10}$$

Substituting Eq. (3.3.10) into Eq. (3.3.9), and using Eq. (3.2.8) to change the exponent on $\delta_{(2,\perp h)}^{(\max)}$ and rewrite the coefficient, we find,

$$\delta_{(2,\perp h)}^{(\max)} = \left[{}_3\mathfrak{P}_{\perp h}^{(1)}\frac{s_3}{s_2}\right]^{1/s_3}\delta_{(3)}^{(\max)}. \tag{3.3.11}$$

Because we must have

$$\delta_{(2,\perp h)}^{(\max)} \le \delta_{(3)}^{(\max)}, \quad \text{then} \quad {}_3\mathfrak{P}_{\perp h}^{(1)}\frac{s_3}{s_2}\le 1 \quad \text{and} \quad {}_3\mathfrak{P}_{\perp h}^{(1)}\le\frac{s_2}{s_3}. \tag{3.3.12}$$

Thus in a horizontal sampling plane that is perpendicular to **h** and is randomly placed in the volume $\mathcal{V}$, the probability ${}_3\mathfrak{P}_{\perp h}^{(1)}$ that the maximum displacement observed is actually the maximum displacement in the volume is no greater than s_2/s_3.

3.4. Constraints on the size of the sampling volume relative to the largest included fault

From Eqs. (3.3.8)$_3$ and (3.3.12)$_3$ we can derive distinct limits on the minimum size of the volume $\mathcal{V}$ that must be used for adequate sampling of the faults, or conversely on the maximum size of the largest fault that can be included in this type of strain analysis for a given sized volume. Introducing Eq. (3.1.22)$_1$ with (2.1.9)$_1$ into Eq. (3.3.8)$_3$, and introducing Eq. (3.1.22)$_3$ into Eq. (3.3.12)$_3$, we find,

$${}_3\mathfrak{P}_t^{(1)} = \frac{\lambda\left(L^{(1)}\right)^2\cos\theta}{\mathcal{W}\mathcal{H}}\le\frac{s_1}{s_3}, \quad {}_3\mathfrak{P}_{\perp h}^{(1)} = \frac{\mu L^{(1)}\sin\rho}{\mathcal{H}}\le\frac{s_2}{s_3}. \tag{3.4.1}$$

The inequalities in Eqs. (3.4.1) give,

$$\mathcal{W}\mathcal{H}\ge\frac{s_3}{s_1}\lambda\left(L^{(1)}\right)^2\cos\theta, \quad \mathcal{H}\ge\frac{s_3}{s_2}\mu L^{(1)}\sin\rho. \tag{3.4.2}$$

Looking first at Eq. (3.4.2)$_1$, we know from Eq. (2.1.13)$_1$ that $\lambda(L^{(1)})^2$ is the area of the largest fault, and thus $\lambda(L^{(1)})^2\cos\theta$ is the area of that fault projected onto a plane normal to the transect line **t**. From Equation (3.2.6), we also know that $s_1<s_3$. Thus Eq. (3.4.2)$_1$ says that the cross-sectional area WH of the volume $\mathcal{V}$ measured normal to the transect line **t** is at least $(s_3/s_1)>1$ times the area of the largest fault projected on a plane normal to **t**.

Looking next at Eq. (3.4.2)$_2$, we know from Eq. (3.1.21) that $\mu L^{(1)}=l^{(1)}$ is the down-dip width of the largest fault and $\mu L^{(1)}\sin\rho$ is therefore the vertical extent of the largest fault. From Equation (3.2.8), we also know that $s_2<s_3$. Thus Eq. (3.4.2)$_2$ says that the vertical dimension $\mathcal{H}$ of the volume $\mathcal{V}$ should be at least $(s_3/s_2)>1$ times the vertical dimension of the largest fault. Equations (3.4.2) are independent constraints on the size of $\mathcal{V}$, which therefore must apply for all possible values of $\mathcal{H}$. The minimum possible value of $\mathcal{H}$ is given by the equality in Eq. (3.4.2)$_2$. If we substitute this value for $\mathcal{H}$ into Eq. (3.4.2)$_1$, we find,

$$\mathcal{W}\ge\frac{s_2}{s_1}\frac{\lambda}{\mu}\frac{\cos\theta}{\sin\rho}L^{(1)}. \tag{3.4.3}$$

We note, from Eqs. (2.1.13)$_2$ and (3.1.21)$_2$, that for a rectangular fault, $\lambda/\mu=1$. To simplify the estimate of the horizontal width $\mathcal{W}$ of the volume $\mathcal{V}$, we therefore assume a rectangular, vertical ($\rho=90^\circ$) fault and a traverse direction **t** perpendicular to that fault ($\theta=0^\circ$). With these assumptions, Eqs. (3.4.2)$_2$ and (3.4.3) give,

$$\left.\begin{array}{l}\text{for}\quad \dfrac{\lambda}{\mu}=1,\quad \theta=0^\circ,\quad \text{and}\quad \rho=90^\circ,\\ \mathcal{W}\ge\dfrac{s_2}{s_1}L^{(1)},\quad \mathcal{H}\ge\dfrac{s_3}{s_2}\mu L^{(1)}=\dfrac{s_3}{s_2}l^{(1)}.\end{array}\right\} \tag{3.4.4}$$

Because $s_1<s_2<s_3$ (Eqs. (3.2.6) and (3.2.8)), the dimensions of the volume $\mathcal{V}$ must be larger than those of the largest vertical-equivalent-fault that can be included in an analysis using fault systematics.

Thus, for an analysis that relies on the relations of fault systematics, Equations (3.4.2)–(3.4.4) prescribe, for a given size of the largest fault, how large a volume we must consider in order for the analysis to be valid. Conversely, for a volume of a given size, these equations prescribe the largest fault that can be included in this type of analysis.

We can express these constraints in terms of the maximum displacement on the largest fault. Introducing Eq. (3.1.1) for the largest fault into the inequalities in Eq. (3.4.4) gives,

$$\left.\begin{array}{l}\text{for}\quad \dfrac{\lambda}{\mu}=1,\quad \theta=0^\circ,\quad \text{and}\quad \rho=90^\circ,\\ \mathcal{W}\ge\dfrac{s_2}{s_1}B^{\frac{1}{p}}\left(\delta_{(3)}^{(\max)}\right)^{\frac{1}{p}},\quad \mathcal{H}\ge\dfrac{s_3}{s_2}\mu B^{\frac{1}{p}}\left(\delta_{(3)}^{(\max)}\right)^{\frac{1}{p}}.\end{array}\right\} \tag{3.4.5}$$

In the companion paper (Part II, Section 3) we use the empirical results for the constants p, B, and s_ζ to give quantitative estimates for these constraints.

4. Estimation of infinitesimal strains using fault population systematics: summary and comparison of results for three-, two-, and one-dimensional sampling domains

We can apply fault population systematics to the estimation of infinitesimal extension and shear strain in two specific circumstances for which sampling is incomplete. In the first case, sampling resolution is incomplete, and we determine the total strains for a local domain in which we systematically have studied only the larger faults, and we need to account for the contributions of the smaller unsampled faults. We assume we have measured the displacement $\delta_{(\zeta,v)}^{(\max)}$ on the largest fault, and we use the

equation for the cumulative frequency of fault-displacement (Eq. (3.1.11)) to determine the contribution of the smaller faults to the total strain. In the second case, sampling of the spatial extent of the domain is incomplete, and we use the equation for the cumulative frequency of fault-displacement to determine the strain for a regional domain when our observations are limited to a local domain that does not span the regional domain, and we need to determine the effects of both the larger and the smaller faults.

Both cases require the assumption that the power-law scaling relationship for the cumulative frequency of the displacement is valid for faults of all sizes, both observed and unobserved, and that the same equation applies throughout the domain, i.e. that the faults are homogeneously distributed in the domain. Moreover, in practice one also must make some estimate for the limit of the power-law distribution at large displacements where the frequency curve falls off from the power-law model (Fig. 3B; see also Fig. II:4C in the companion paper, Part II). Without such a limit, the power-law model would overestimate the strain. This modification to the theory for practical applications is discussed by Marrett (1996), and it will not be included in the analysis in this paper.

In Section 4.1, we summarize the derivations of the strain equations for the first case, considering local sampling domains having three, two, and one spatial dimensions. We show that we can estimate the total strain in a local domain if we know the slope of the displacement–frequency curve and the displacement on the largest fault in the domain, which constrains the intercept for the log-linear cumulative frequency line by Eqs. $(3.3.1)_2$, $(3.3.2)_2$, or $(3.3.3)_2$. Details of the derivations for the domains of three, two, and one dimensions are given in the Supplementary Material, Sections S1, S2, and S3, respectively.

The equations differ for sampling domains having a different number of dimensions because the scale factor that defines the contribution of a specific fault to the strain of a domain is different. Therefore in Sections 4.2 and 4.3, we examine how these different equations are related and how we can constrain the three-dimensional strain from sampling in either two dimensions (Section 4.2) or one dimension (Section 4.3). In Section 4.4, we then indicate how we can make estimates of strain for the second case in which sampling of the spatial extent of the domain is incomplete, and the domain of interest is larger than the sampling domain.

4.1. Equations for strain from sampling in domains of different dimensionality: summary of derivations

For a given spatial domain, the extensional strain that is contributed by the ith fault within that domain is, for three, two, and one dimensions, a weighting factor times the local extension due to slip on the fault. The weighting factor is different for each dimensionality and is determined by the size of the fault relative to the domain. In summarizing these equations below, we list on the left the equation numbers, mostly from the detailed derivation in the Supplementary Material, and on the right, we give an equation number for convenient reference to this section.

The extensional strain parallel to **t** that is contributed to the sampling domain by the ith fault is given for a three-, two-, and one-dimensional sampling domain by the respective relations,

$$(S1.1.4)\quad e^{(i)}_{(3,t)} = {}_3\mathfrak{P}^{(i)}_t\left[\frac{\delta^{(i)}\cos\phi}{\mathcal{T}}\right], \tag{4.1.1}$$

$$(S2.1.3)\quad e^{(i)}_{(2,t)} = {}_2\mathfrak{P}^{(i)}_t\left[\frac{\delta^{(i)}\cos\phi}{\mathcal{T}}\right], \tag{4.1.2}$$

$$(S3.1.1)\quad e^{(i)}_{(1,t)} = {}_1\mathfrak{P}^{(i)}_t\left[\frac{\delta^{(i)}\cos\phi}{\mathcal{T}}\right]. \tag{4.1.3}$$

The shear strains for a pair of orthogonal lines parallel to **t** and **w** are given by the equations,

$$(S1.1.5)\quad e^{(i)}_{(3,\gamma)} = \frac{1}{2}\left\{{}_3\mathfrak{P}^{(i)}_t\left[\frac{\delta^{(i)}\cos\beta}{\mathcal{T}}\right] + {}_3\mathfrak{P}^{(i)}_w\left[\frac{\delta^{(i)}\cos\phi}{\mathcal{W}}\right]\right\}, \tag{4.1.4}$$

$$(S2.1.4)\quad e^{(i)}_{(2,\gamma)} = \frac{1}{2}\left\{{}_2\mathfrak{P}^{(i)}_t\left[\frac{\delta^{(i)}\cos\beta}{\mathcal{T}}\right] + {}_2\mathfrak{P}^{(i)}_w\left[\frac{\delta^{(i)}\cos\phi}{\mathcal{W}}\right]\right\}, \tag{4.1.5}$$

$$(S3.1.2)\quad e^{(i)}_{(1,\gamma)} = \frac{1}{2}\left\{{}_1\mathfrak{P}^{(i)}_t\left[\frac{\delta^{(i)}\cos\beta}{\mathcal{T}}\right] + {}_1\mathfrak{P}^{(i)}_w\left[\frac{\delta^{(i)}\cos\phi}{\mathcal{W}}\right]\right\}. \tag{4.1.6}$$

The weighting factor ${}_\zeta\mathfrak{P}^{(i)}_v$ in each equation is the probability that the ith fault (superscript) in a ζ-dimensional domain (left subscript) is intersected by a randomly located line through the domain oriented parallel to **t** or **w** (as indicated by the right subscript $v = t$ or w, respectively). The probability is a ratio, for which the numerator is the projected size of the ith fault, and the denominator is the projected size of the sampling domain. For $\zeta = 3$, the size of the fault is its area projected onto a plane normal to the direction **t** (or **w**), and the size of the sampling domain is the cross-sectional area of the domain on the same plane; for $\zeta = 2$, the size of the fault is the length of the fault line in the sampling plane projected onto a line normal to the direction **t** (or **w**), and the size of the sampling domain is the length of the domain normal to **t** (or **w**); for $\zeta = 1$, any fault in the domain cuts completely through the domain, so the probability is 1. Expressions for the probabilities in each of the above equations, expressed in terms of the displacement, are,

$$(3.1.22)_2,(3.1.29)_2,(S1.1.3)_2\quad {}_3\mathfrak{P}^{(i)}_t = \frac{\lambda B^{2/p}\cos\theta}{\mathcal{A}_t}\left(\delta^{(i)}\right)^{2/p},$$

$${}_3\mathfrak{P}^{(i)}_w = \frac{\lambda B^{2/p}\cos\alpha}{\mathcal{A}_w}\left(\delta^{(i)}\right)^{2/p}, \tag{4.1.7}$$

$$(S2.1.20)\quad {}_2\mathfrak{P}^{(i)}_t = \frac{\nu^{(i)}B^{1/p}\cos\theta}{\mathcal{W}\sin\rho}\left(\delta^{(i)}\right)^{1/p},$$

$${}_2\mathfrak{P}^{(i)}_w = \frac{\nu^{(i)}B^{1/p}\cos\alpha}{\mathcal{T}\sin\rho}\left(\delta^{(i)}\right)^{1/p}, \tag{4.1.8}$$

$$(S3.1.5)\quad {}_1\mathfrak{P}^{(i)}_t = 1, \quad \text{and} \quad {}_1\mathfrak{P}^{(i)}_w = 1. \tag{4.1.9}$$

In Eq. (4.1.8), $\nu^{(i)}$ are geometric factors defined by

$$(S2.1.17)\quad \nu^{(i)} \equiv \frac{\overline{L}^{(i)}}{L^{(i)}} = \frac{A^{(i)}/\ell^{(i)}}{L^{(i)}} = \frac{A^{(i)}}{\ell^{(i)}L^{(i)}} \tag{4.1.10}$$

where $\overline{L}^{(i)}$ is the average length of the ith fault trace on random horizontal planes through the volume that cut the fault, $L^{(i)}$ is the maximum horizontal length of the fault, $A^{(i)}$ is the actual area of the ith fault, and $\ell^{(i)}$ is the maximum down-dip width of the fault. $\nu^{(i)}$ therefore accounts, on average, for the effect of the shape of the fault tip line on the apparent length of the fault trace in the horizontal sampling plane. It has a value of 1 for a rectangular fault.

Substituting Eqs. (4.1.7)–(4.1.9) into Eqs. (4.1.1)–(4.1.6), we find that for the three- and two-dimensional sampling domains, the equations for extension and for shear strain in the same domain have similar forms, differing only by the constant terms. Thus, if we let 'x' in the subscripts stand for either 't' or 'γ', we can write the equations in compact form as,

$$(\text{S1.1.10}) \quad e^{(i)}_{(3,x)} = \frac{D_{(3,x)}}{\mathcal{V}}\left(\delta^{(i)}\right)^{(1+2/p)}, \tag{4.1.11}$$

$$(\text{S2.1.23}) \quad e^{(i)}_{(2,x)} = \frac{D_{(2,x)}}{\mathcal{T}\mathcal{W}}\left(\delta^{(i)}\right)^{(1+1/p)}, \tag{4.1.12}$$

$$(\text{S3.1.6}) \quad \left.\begin{aligned} e^{(i)}_{(1,t)} &= \left(\frac{\cos\phi}{\mathcal{T}}\right)\delta^{(i)}, \\ e^{(i)}_{(1,\gamma)} &= \tfrac{1}{2}\left[\left(\frac{\cos\beta}{\mathcal{T}}\right)\delta^{(i)} + \left(\frac{\cos\phi}{\mathcal{W}}\right)\delta^{(i)}\right], \end{aligned}\right\} \tag{4.1.13}$$

The constants $D_{(3,x)}$ and $D_{(2,x)}$ are defined by,

$$(\text{S1.1.8}),(\text{S1.1.9}) \quad \left.\begin{aligned} D_{(3,t)} &\equiv \lambda B^{2/p}(\cos\theta\cos\phi), \\ D_{(3,\gamma)} &\equiv 0.5\lambda B^{2/p}(\cos\theta\cos\beta + \cos\phi\cos\alpha), \end{aligned}\right\} \tag{4.1.14}$$

$$(\text{S2.1.22}) \quad \left.\begin{aligned} D_{(2,t)} &\equiv \frac{\nu B^{1/p}}{\sin\rho}\cos\theta\cos\phi, \\ D_{(2,\gamma)} &\equiv \frac{\nu B^{1/p}}{2\sin\rho}[\cos\theta\cos\beta + \cos\alpha\cos\phi]. \end{aligned}\right\} \tag{4.1.15}$$

We do not define D for the case of one-dimensional sampling, because to obtain the total shear strain from Eq. $(4.1.13)_2$, we must sum the two terms in the equation over different sets of faults: one set comprises faults intersected by a line parallel to **t**; the other set comprises faults intersected by a line parallel to **w**, which is orthogonal to **t**. Sampling in these two directions means that the total shear strain involves two different distributions, whereas the extension (Eq. $(4.1.13)_1$) involves only one distribution. Thus the two Eqs. (4.1.13) may not both be simplified to a scale-independent constant D times a single variable.

The expressions for the differential of the strain component are derived by assuming that the discrete strain contributed by one fault is in general a very small part of the total strain. We therefore can treat the discrete increments of strain described in Eqs. (4.1.1)–(4.1.6) as differentials of continuous functions, which are defined in terms of a continuous displacement variable δ and the differential of a continuous cumulative number distribution $dN(\delta)$ that defines the displacement distribution in the sampling domain. Using Eq. (3.1.13), the continuous cumulative number distribution can be converted to a continuous cumulative frequency distribution $df(\delta)$. The continuous-function descriptions are,

$$(\text{S1.1.12}) \quad de_{(3,x)}(\delta) = D_{(3,x)}\delta^{(1+2/p)}\, df_3(\delta), \tag{4.1.16}$$

$$(\text{S2.1.25}) \quad de_{(2,x)}(\delta) = D_{(2,x)}\delta^{(1+1/p)}\, df_{(2,\perp h)}(\delta), \tag{4.1.17}$$

$$(\text{S3.1.9}) \quad \left.\begin{aligned} de_{(1,t)}(\delta) &= \delta\cos\phi\, df_{(1,t)}(\delta), \\ de_{(1,\gamma)}(\delta) &= 0.5\left\{\delta\cos\beta\, df_{(1,t)}(\delta) + \delta\cos\phi\, df_{(1,w)}(\delta)\right\} \end{aligned}\right\} \tag{4.1.18}$$

The different distributions, $df_{(1,t)}(\delta)$ and $df_{(1,w)}(\delta)$, required for determining the shear strain with one-dimensional sampling become explicit in Eq. $(4.1.18)_2$. Then using Eq. $(3.1.14)_2$, we find,

$$(\text{S1.1.13}) \quad de_{(3,x)} = -D_{(3,x)}s_3 r_{(3)}\delta^{-(s_3-2/p)}\, d\delta, \tag{4.1.19}$$

$$(\text{S2.1.27}) \quad de_{(2,x)} = -D_{(2,x)}s_2 r_{(2,\perp h)}\delta^{-(s_2-1/p)}\, d\delta, \tag{4.1.20}$$

$$(\text{S3.1.10}) \quad \left.\begin{aligned} de_{(1,t)}(\delta) &= -s_1 r_{(1,t)}\cos\phi\,\delta^{-s_1}\, d\delta, \\ de_{(1,\gamma)}(\delta) &= -0.5s_1\left[r_{(1,t)}\cos\beta + r_{(1,w)}\cos\phi\right]\delta^{-s_1}\, d\delta. \end{aligned}\right\} \tag{4.1.21}$$

All the Equations (4.1.19)–(4.1.21) for the differential of the extension are actually the same, although each is expressed in terms of the variables pertinent to the number of dimensions in the specific sampling domain (see Supplementary Material Sections S1.1, S2.2, S3.2). The same statement also applies to the differentials of the shear strain. This identity is apparent because from Eqs. (3.2.6) and (3.2.8), the exponents on the displacement are all equal, and we can easily show, using Eqs. (4.1.14) and (4.1.15) with Eqs. (3.2.6)–(3.2.9) that,

$$\left.\begin{aligned} D_{(3,t)}s_3 r_{(3)} &= D_{(2,t)}s_2 r_{(2,\perp h)} = 0.5\cos\phi\, s_1 r_{(1,t)}, \\ D_{(3,\gamma)}s_3 r_{(3)} &= D_{(2,\gamma)}s_2 r_{(2,\perp h)} = 0.5\cos\beta\, s_1 r_{(1,t)} + 0.5\cos\phi\, s_1 r_{(1,w)}. \end{aligned}\right\} \tag{4.1.22}$$

We can also derive Eqs. (4.1.20) and (4.1.21) directly from Eq. (4.1.19) (for details, see the Supplementary Material, Sections S2.1, S2.2, S3.1, and S3.2). These derivations demonstrate the consistency of the definitions of the probabilities in Eqs. (4.1.7)–(4.1.9).

The cumulative strain contributed by all faults having displacements greater than or equal to δ is given by the integrals of Eqs. (4.1.19)–(4.1.21),

$$(\text{S1.2.1}) \quad e^{(\text{cum})}_{(3,x)}(\delta) = \int_{\mathcal{V}} de_{(3,x)}(\delta) = -D_{(3,x)}s_3 r_{(3)} \int_{\mathcal{V}} \delta^{-(s_3-2/p)}\, d\delta, \tag{4.1.23}$$

$$(\text{S2.3.1}) \quad e^{(\text{cum})}_{(2,x)}(\delta) = \int_{\mathcal{A}_h} de_{(2,x)}(\delta) = -D_{(2,x)}s_2 r_{(2,\perp h)} \int_{\mathcal{A}_h} \delta^{-(s_2-1/p)}\, d\delta, \tag{4.1.24}$$

$$(\text{S3.4.1}) \quad e^{(\text{cum})}_{(1,t)}(\delta) = \int_{\mathcal{T}} de_{(1,t)}(\delta) = -s_1 r_{(1,t)}\cos\phi \int_{\mathcal{T}} \delta^{-s_1}\, d\delta, \tag{4.1.25}$$

$$(\text{S3.4.11}) \quad e^{(\text{cum})}_{(1,\gamma)}(\delta) = \int_{\mathcal{T},\mathcal{W}} de_{(1,\gamma)}(\delta) = \frac{1}{2}\left[-s_1 r_{(1,t)}\cos\beta \times \left(\int_{\mathcal{T}} \delta^{-s_1}\, d\delta\right) - s_1 r_{(1,w)}\cos\phi \times \left(\int_{\mathcal{W}} \delta^{-s_1}\, d\delta\right)\right]. \tag{4.1.26}$$

where the symbols below the integral signs identify the domain for which the strain is determined. Taking the indefinite integrals gives,

$$(\text{S1.2.2})\quad e^{(\text{cum})}_{(3,x)}(\delta) = -D_{(3,x)} s_3 r_{(3)} \left[\frac{\delta^{[1-(s_3-2/p)]}}{1-(s_3-2/p)} + C_{(3)} \right], \qquad (4.1.27)$$

$$(\text{S2.3.2})\quad e^{(\text{cum})}_{(2,x)}(\delta) = -D_{(2,x)} s_2 r_{(2,\perp h)} \left[\frac{\delta^{[1-(s_2-1/p)]}}{1-(s_2-1/p)} + C_{(2,\perp h)} \right], \qquad (4.1.28)$$

$$(\text{S3.4.2})\quad e^{(\text{cum})}_{(1,t)}(\delta) = -s_1 r_{(1,t)} \cos\phi \left[\frac{\delta^{(1-s_1)}}{(1-s_1)} + C_{(1,t)} \right], \qquad (4.1.29)$$

$$(\text{S3.4.12})\quad e^{(\text{cum})}_{(1,\gamma)}(\delta) = \frac{1}{2}\left[-s_1 r_{(1,t)} \cos\beta \left(\frac{\delta^{(1-s_1)}}{(1-s_1)} + K_{(1,t)} \right) - s_1 r_{(1,w)} \cos\phi \left(\frac{\delta^{(1-s_1)}}{(1-s_1)} + K_{(1,w)} \right) \right]. \qquad (4.1.30)$$

The constants of integration are evaluated in each case in terms of the largest displacement in each sample by setting the left side of Eqs. (4.1.27)–(4.1.30) equal to the extension and shear strain contributed by the largest fault in each sample. These extensions and shear strains are determined by setting $i = 1$ in Eqs. (4.1.1)–(4.1.6), for which

$$\delta = \delta^{(i)}\big|_{i=1} = \delta^{(1)}_{(\zeta,\nu)} = \delta^{(\max)}_{(\zeta,\nu)}. \qquad (4.1.31)$$

Eqs. (3.3.7) and (3.3.11) show that these maximum displacements are in general different for sampling domains of different dimensionality, and that the largest fault in a lower-dimensioned sampling domain can be smaller, and can have a smaller displacement, than the largest fault in the volume.

Evaluating the constants of integration from these constraints, we find,

$$(\text{S1.2.6})\quad C_{(3)} = -\left(\delta^{(\max)}_{(3)}\right)^{[1-(s_3-2/p)]} \left[\frac{1+2/p}{s_3[1-(s_3-2/p)]} \right], \qquad (4.1.32)$$

$$(\text{S2.3.7})\quad C_{(2,\perp h)} = -\left(\delta^{(\max)}_{(2,\perp h)}\right)^{[1-(s_2-1/p)]} \left[\frac{1+1/p}{s_2[1-(s_2-1/p)]} \right], \qquad (4.1.33)$$

$$(\text{S3.4.7})\quad C_{(1,t)} = -\left(\delta^{(\max)}_{(1,t)}\right)^{(1-s_1)} \left(\frac{1}{s_1(1-s_1)} \right), \qquad (4.1.34)$$

$$(\text{S3.4.17})\quad \left.\begin{aligned} K_{(1,t)} &= -\left(\delta^{(\max)}_{(1,t)}\right)^{(1-s_1)} \left[\frac{1}{s_1(1-s_1)} \right], \\ K_{(1,w)} &= -\left(\delta^{(\max)}_{(1,w)}\right)^{(1-s_1)} \left[\frac{1}{s_1(1-s_1)} \right] \end{aligned}\right\} \qquad (4.1.35)$$

Introducing these constants from Eqs. (4.1.32)–(4.1.35) into the integrated Eqs. (4.1.27)–(4.1.30), gives the cumulative strains as a function of the displacement:

$$(\text{S1.2.7})\quad e^{(\text{cum})}_{(3,x)}(\delta) = e^{(1)}_{(3,x)} \left[\left(\frac{1+2/p}{1-(s_3-2/p)} \right) - \frac{s_3}{1-(s_3-2/p)} \left(\frac{\delta}{\delta^{(\max)}_{(3)}} \right)^{[1-(s_3-2/p)]} \right], \qquad (4.1.36)$$

$$(\text{S2.3.9})\quad e^{(\text{cum})}_{(2,x)}(\delta) = e^{(1)}_{(2,x)} \left[\left(\frac{1+1/p}{1-(s_2-1/p)} \right) - \frac{s_2}{[1-(s_2-1/p)]} \left(\frac{\delta}{\delta^{(\max)}_{(2,\perp h)}} \right)^{[1-(s_2-1/p)]} \right], \qquad (4.1.37)$$

$$(\text{S3.4.8})\quad e^{(\text{cum})}_{(1,t)}(\delta) = e^{(1)}_{(1,t)} \left[\frac{1}{1-s_1} - \frac{s_1}{1-s_1} \left(\frac{\delta}{\delta^{(\max)}_{(1,t)}} \right)^{(1-s_1)} \right], \qquad (4.1.38)$$

$$(\text{S3.4.19})\quad e^{(\text{cum})}_{(1,\gamma)}(\delta) = \frac{1}{2} \sum_{\nu=t,w} e^{(1)}_{(1,\gamma\nu)} \left[\frac{1}{(1-s_1)} - \frac{s_1}{(1-s_1)} \left(\frac{\delta}{\delta^{(\max)}_{(1,\nu)}} \right)^{(1-s_1)} \right]. \qquad (4.1.39)$$

The shear strains $e^{(1)}_{(1,\gamma\nu)}$ that appear in Eq. (4.1.39) under the summation over $\nu = t,w$, are due to the displacements $\delta^{(\max)}_{(1,t)}$ and $\delta^{(\max)}_{(1,w)}$ which occur on the largest fault intersected by the sampling lines parallel to **t** and **w**, respectively. These shear strain components define, respectively, the shear of the line parallel to **t** in the direction **w**, and the shear strain of the line parallel to **w** in the direction **t** (see the Supplementary Material, Eq. (S3.4.20)).

Because each of Eqs. (4.1.37)–(4.1.39) is the cumulative strain due to faults having displacements between $\delta^{(\max)}_{(\zeta,\nu)}$ and δ, we find the total strain by setting $\delta = 0$.

$$(\text{S1.2.8})\quad e^{(\text{tot})}_{(3,x)} = e^{(1)}_{(3,x)} \left(\frac{1+2/p}{1-(s_3-2/p)} \right), \qquad (4.1.40)$$

$$(\text{S2.3.10})\quad e^{(\text{tot})}_{(2,x)} = e^{(1)}_{(2,x)} \left(\frac{1+1/p}{1-(s_2-1/p)} \right), \qquad (4.1.41)$$

$(\text{S3.4.9}),(\text{S3.4.22})_2,(\text{S3.4.23})$

$$\left.\begin{aligned} e^{(\text{tot})}_{(1,t)} &= e^{(1)}_{(1,t)} \left[\frac{1}{1-s_1} \right], \\ e^{(\text{tot})}_{(1,\gamma)} &= 0.5 \sum_{\nu=t,w} e^{(1)}_{(1,\gamma\nu)} \frac{1}{(1-s_1)} = e^{(1)}_{(1,\gamma)} \frac{1}{(1-s_1)}. \end{aligned}\right\} \qquad (4.1.42)$$

Note that because of Eqs. (3.2.6) and (3.2.8), the denominator on the right of each of the equations (4.1.40)–(4.1.42) equals $(1-s_1)$. Thus the equations differ in the numerator and in the strain contributed by the largest fault in the domain, which in turn depends on the magnitude of the probability defined in Eqs. (4.1.7)–(4.1.9).

It is of interest to know what proportion of the extension or shear strain in the given direction is contributed by the largest fault, and what proportion is contributed by all the smaller faults. We evaluate the ratio of the strain component contributed by the largest fault to the total strain component by rearranging Eq. (4.1.40) to find

$$\frac{e^{(1)}_{(3,x)}}{e^{(\text{tot})}_{(3,x)}} = \frac{p+2-s_3 p}{p+2} = \frac{p+2-m_3}{p+2}, \qquad (4.1.43)$$

where we used Eq. (3.1.9)$_1$ with $\zeta = 3$ to find the second relation. The ratio in Eq. (4.1.43) must be greater than zero, because the ratio must be positive; and it must be less than 1, because the largest fault cannot account for more than all the extension. Thus,

$$0 < \frac{e^{(1)}_{(3,x)}}{e^{(\mathrm{tot})}_{(3,x)}} = \frac{p+2-s_3 p}{p+2} \le 1, \tag{4.1.44}$$

This implies the following constraints on the possible values of the parameters relative to one another,

$$0 \le s_3 < 1 + 2/p, \quad 0 \le s_2 < 1 + 1/p, \quad 0 \le s_1 < 1, \tag{4.1.45}$$

where the second two equations come from the first by using Eqs. (3.2.6) and (3.2.8). We can use Eq. (3.1.9)$_1$ to express Eq. (4.1.45)$_1$ in terms of m_ζ, which leads to the constraints,

$$0 \le m_3 < p+2, \quad 0 \le m_2 < p+1, \quad 0 \le m_1 < p, \tag{4.1.46}$$

where the second two equations come from the first using Eqs. (3.2.2) and (3.2.4). Eqs. (4.1.46) also imply,

$$p > m_3 - 2, \quad p > m_2 - 1, \quad p > m_1. \tag{4.1.47}$$

The cumulative strains are conveniently expressed as a fraction of the total strains by dividing the cumulative strains in Eqs. (4.1.36)–(4.1.39) by the appropriate total strains from Eqs. (4.1.40)–(4.1.42):

$$(\mathrm{S1.2.10})_1 \quad \frac{e^{(\mathrm{cum})}_{(3,x)}(\delta)}{e^{(\mathrm{tot})}_{(3,x)}} = 1 - \frac{s_3 p}{p+2}\left(\frac{\delta}{\delta^{(\max)}_{(3)}}\right)^{[1-(s_3-2/p)]}, \tag{4.1.48}$$

$$(\mathrm{S2.3.12})_1 \quad \frac{e^{(\mathrm{cum})}_{(2,x)}(\delta)}{e^{(\mathrm{tot})}_{(2,x)}} = 1 - \frac{s_2 p}{p+1}\left(\frac{\delta}{\delta^{(\max)}_{(2,\perp h)}}\right)^{[1-(s_2-1/p)]}, \tag{4.1.49}$$

$$(\mathrm{S3.4.10}),(\mathrm{S3.4.25}) \quad \left.\begin{aligned} \frac{e^{(\mathrm{cum})}_{(1,t)}(\delta)}{e^{(\mathrm{tot})}_{(1,t)}} &= 1 - s_1\left[\frac{\delta}{\delta^{(\max)}_{(1,t)}}\right]^{(1-s_1)}, \\ \frac{e^{(\mathrm{cum})}_{(1,\gamma)}(\delta)}{e^{(\mathrm{tot})}_{(1,\gamma)}} &= 1 - \frac{0.5}{e^{(1)}_{(1,\gamma)}}\sum_{v=t,w} e^{(1)}_{(1,\gamma v)}\left(s_1\left[\frac{\delta}{\delta^{(\max)}_{(1,v)}}\right]^{(1-s_1)}\right) \end{aligned}\right\} \tag{4.1.50}$$

Note again that because of Eqs. (3.2.6) and (3.2.8), the exponents on the displacement terms are all equal to $(1 - s_1)$.

The significant difference among the integrated equations for the extensional strains or for the shear strains (Eqs. (4.1.36)–(4.1.39)) is in the evaluation of the constants of integration. Each constant is different because it is evaluated in terms of the strain in each domain that is contributed by the largest fault, identified by setting $i = 1$ in Eqs. (4.1.1)–(4.1.6). This strain in turn depends on a probability ${}_\zeta\mathfrak{P}^{(i)}_\nu$ that a fault will be intersected by the specific sampling domain, and this probability is different for the domains having a different dimensionality. Thus for the different curves that plot the cumulative strain as a function of displacement for domains having a different dimensionality, the anchor points are at different strains, and as a result, the total strain will have different values for the different domains.

Because the cumulative strain must be less than or equal to the total strain, we can use Eq. (4.1.48) to derive the same constraints on the value of s_3 as we found in Eq. (4.1.45) (see the Supplementary Material, Section S4.1)

4.2. Comparison of strains from sampling domains of two and three dimensions

We can compare the total strains for a two-dimensional sampling domain to those for the three-dimensional sampling domain by dividing Eqs. (4.1.41) by Eq. (4.1.40), and using Eqs. (3.2.6) and (3.2.8) to find,

$$(\mathrm{S4.2.2}) \quad \frac{e^{(\mathrm{tot})}_{(2,x)}}{e^{(\mathrm{tot})}_{(3,x)}} = \frac{e^{(1)}_{(2,x)}}{e^{(1)}_{(3,x)}}\left(\frac{p+1}{p+2}\right). \tag{4.2.1}$$

For both the extensional strain ($x = t$) and for the shear strain ($x = \gamma$), we can show (see the Supplementary Material, Section S4.2) that Eq. (4.2.1) implies the constraint,

$$(\mathrm{S4.2.16}) \quad \frac{e^{(\mathrm{tot})}_{(2,x)}}{e^{(\mathrm{tot})}_{(3,x)}} \le \left[\frac{s_3}{s_2}\right]\left(\frac{p+1}{p+2}\right), \tag{4.2.2}$$

where, as before, the subscript 'x' stands for either 't' or 'γ'.

4.3. Comparison of strains from sampling domains of one and three dimensions

We also can compare the total extension inferred from a one-dimensional sampling domain to that inferred from a three-dimensional sampling domain by dividing Eq. (4.1.42)$_1$ by Eq. (4.1.40) with the subscript 'x' set to 't'. Using Eqs. (3.2.6) and (3.2.8), the result simplifies to

$$(\mathrm{S4.3.2}) \quad \frac{e^{(\mathrm{tot})}_{(1,t)}}{e^{(\mathrm{tot})}_{(3,t)}} = \frac{e^{(1)}_{(1,t)}}{e^{(1)}_{(3,t)}}\left[\frac{p}{p+2}\right]. \tag{4.3.1}$$

After some manipulation, we can show (see the Supplementary Material, Section S4.3) that Eq. (4.3.1) leads to the constraint,

$$(\mathrm{S4.3.4}) \quad \frac{e^{(\mathrm{tot})}_{(1,t)}}{e^{(\mathrm{tot})}_{(3,t)}} \le \left[\frac{s_3}{s_1}\right]\left(\frac{p}{p+2}\right). \tag{4.3.2}$$

Finally, we can compare the shear strain inferred from one-dimensional sampling to that for three-dimensional sampling by dividing Eq. (4.1.42)$_2$ by Eq. (4.1.40), using the subscript 'x' set to 'γ'.

$$(\mathrm{S4.4.1}) \quad \frac{e^{(\mathrm{tot})}_{(1,\gamma)}}{e^{(\mathrm{tot})}_{(3,\gamma)}} = \frac{0.5\left(e^{(1)}_{(1,\gamma t)} + e^{(1)}_{(1,\gamma w)}\right)}{e^{(1)}_{(3,\gamma)}}\frac{1}{(1-s_1)}\left(\frac{1+2/p}{1-(s_3-2/p)}\right). \tag{4.3.3}$$

Again after some manipulation, we can show (see the Supplementary Material, Section S4.4) that Eq. (4.3.3) leads to the constraint,

$$(\mathrm{S4.4.8}) \quad \frac{e^{(\mathrm{tot})}_{(1,\gamma)}}{e^{(\mathrm{tot})}_{(3,\gamma)}} \le \left[\frac{s_3}{s_1}\right]^{1/s_1}\left(\frac{p}{p+2}\right). \tag{4.3.4}$$

The constraint on the shear strain in Eq. (4.3.4) is not as stringent as the constraint for the extension in Eq. (4.3.2). The results are different because determining the shear strain from one-dimensional sampling requires two separate samplings along orthogonal lines, which means that two different distributions are required to calculate the shear strain. This results in equations that cannot be factored and condensed to the same extent as the equations for extension, which then results in less stringent constraints.

4.4. Estimating strains in a regional domain from sampling of a local domain

If the sampling of the spatial extent of a regional domain is incomplete, we only can know the displacement on the largest fault in the local domain that has been sampled, which constrains the cumulative frequency curve by Eqs. $(3.3.1)_2$, $(3.3.2)_2$, or $(3.3.3)_2$. That constraint, however, is in general not valid outside the local domain, because there is no guarantee that the fault with the largest displacement within the local domain would be the fault with the largest displacement in the larger regional domain. The equations for calculating the strains in a local domain depend on knowing the maximum displacement on the largest fault within the domain, or the associated contribution of that fault to the strain (Eqs. (4.1.36)–(4.1.39), as well as the subsequent equations derived from these). We can convert these equations to ones appropriate for calculating the strains in a regional domain, in which the largest fault and the associated maximum displacement are unknown, by substituting for the maximum displacement from Eqs. $(3.3.1)_3$, $(3.3.2)_3$, or $(3.3.3)_3$. This substitution replaces the known maximum displacement in a local domain with an estimate for the maximum displacement in the larger regional domain that is based on the displacement – frequency systematics and the size of the regional domain.

This case requires the assumption that the observed frequencies in a relatively small domain provide useful constraints for the slope and intercept (Eq. $(3.1.11)_2$) of the cumulative frequency relation for displacement in a larger domain. It does not account, however, for the observed fall-off from the log-linear systematics that actually characterizes the data for the very largest faults, and using this approach therefore has the potential to overestimate the frequency of the largest faults, with the result that the strain calculations could be unreliable. Marrett (1996) discusses an approach for dealing with the non-linearity at the large fault end of the spectrum.

5. Discussion

The analysis presented here pertains to the situation in which the strains due to faulting in a body of rock are small. This approximation is the basis for the analysis by Kostrov (1974) that leads to Eq. (2.1.1). The restriction to small strains does not imply that displacement on the faults must be small, however. Even a large displacement on a fault accommodates only a small strain if it is averaged over a volume of rock $\mathcal{V}$ that is large relative to the geometric moment M_0, which is the product of the area of the fault and the displacement on the fault (Eq. (2.1.2)). This is obvious from Eq. (2.1.1), which shows that the strain depends on the ratio $M_0/\mathcal{V}$. We have also assumed that block rotation has a negligible effect on the analysis. Twiss and coworkers have used continuum micropolar theory to account for the effects of block rotation on the slip directions on faults (Twiss et al., 1991, 1993; Twiss, 2009). Their analysis shows that block rotations can affect the slip direction pattern for a set of faults with a diverse distribution of orientations, and thus can affect the strain inferred from such faults. We have not incorporated these rotational effects in this analysis.

Small strains are not necessarily appropriate in all situations. Analysis of the case for finite strain would require that we abandon Eqs. (2.1.1) and (2.1.11), which underlie our entire analysis, and that we formulate the problem in terms of the inverse finite strain, for which the reference length of a deformed line is the deformed length. Finite strains can also give rise to finite block rotations, which change the slip vectors on faults as they rotate (see Fig. 6 in Twiss et al., 1991). Generalization to include finite strain and rotation would add substantially to the complication of the analysis, and we have not ventured into these waters.

Eqs. (4.1.40)–(4.1.42) may not in fact be the best way to estimate the total extension or shear strain in a volume, because they ignore the commonly large deviations from a power-law distribution at the high ends of the length or displacement *vs* cumulative frequency distributions (Fig. 3B; in the companion paper, Part II, see also Figs. II:2 and II:4). The deviation at the lower limit of length or displacement contributes negligibly to the cumulative strain and thus can be ignored. But the deviation from the power-law at the upper end of the displacement distribution would result in Eqs. (4.1.40)–(4.1.42) providing incorrect estimates of the extension or shear strain components in a volume. A better estimate can be found (Marrett and Allmendinger, 1991, 1992; Marrett, 1996) by numerically summing the displacements for the largest faults, and then using Eqs. (4.1.40)–(4.1.42) with $\delta_{(\zeta,v)}^{(\max)}$ equal to the largest of the unsummed displacements to estimate the contribution from all the smaller faults. This technique must also be used if the sampling volume includes faults whose dimensions exceed the limits imposed by the dimensions of the volume itself, as defined by Eqs. (3.4.2) and (3.4.3). In this case, only the strain contributed by faults smaller than this limiting size can be estimated with Eqs. (4.1.40)–(4.1.42); the effect of larger faults must be added individually.

The sampling in one- or two-dimensional domains in general only places constraints on the strain of the three-dimensional volume (Eqs. (4.2.2), (4.3.2), and (4.3.4)). This result is in part because the volume can always contain a larger fault than is present in any given lower-dimensional sampling domain, and in part because the scaling of the contribution of individual fault-displacements to the strain is different for domains having different dimensionality. If, however, the sampling in lower-dimensional domains includes the largest fault in the volume, then the equalities of Eqs. (4.2.2) and (4.3.2) apply, and the extensional and shear strains of the volume are determined exactly from the extensional and shear strains of a two-dimensional domain (Eq. (4.2.2)) and from the extensional strain of a one-dimensional domain (Eq. (4.3.2)). The equality does not apply, however, for the shear strain determined from a one-dimensional domain (Eq. (4.3.4)), so in this case, only a lower bound is determined for the shear strain of the volume.

This approach of using scaling systematics is of major importance for approximating not only the strain, but also other important aggregate characteristics of fractured rock (Marrett, 1996). Thus the scale invariance of faults and fractures and their characteristics, in principle permits the estimation of the aggregate properties of the rock. An accurate estimation of these properties, however, requires a knowledge of the parameters that define the power-law distribution of these characteristics, and a theory for how to use that distribution to calculate the aggregate properties.

6. Summary

The overall problem we address in this paper is how to infer the extension and shear strain in a volume of the brittle crust from observation of fault-displacements or fault-lengths on an incomplete set of faults in a fault system. We encounter two main

problems: The first is how to account for all the faults when any survey of faults in a domain must inevitably be incomplete, due to incomplete exposure and insufficient time for an exhaustive survey. The second is the impossibility of thoroughly sampling a three-dimensional volume of rock because physical access is limited to outcrop on an essentially two-dimensional surface, or to essentially one-dimensional traverses, tunnels, or drill core, and because seismic surveying provides limited resolution. Thus, we need to compensate for incomplete sampling of fault populations, and we need to determine how to infer the strain of a three-dimensional domain from observation of lower-dimensional domains.

The incomplete sampling can be accounted for by using empirical power-laws that describe both the relationship between fault-length and fault-displacement, and the individual cumulative frequency distributions for fault-length and fault-displacement. To that end, we develop the equations for the frequency distributions of fault-displacement and fault-length as they pertain to sampling in three-, two-, and one-dimensional domains, and we derive the relations among these different distributions.

We then derive equations that apply the fault population systematics to the problem of estimating the continuum extension and shear strain in domains of three, two, and one dimensions. The equations are different for domains having a different number of dimensions, and we derive the relationships among the equations for these different dimensionalities. These relations allow us to calculate the total extension or shear strain within the sampled domain knowing only the parameters defining the population systematics and the magnitude of displacement, or the length, of the largest fault in the domain.

We show how the strains inferred from sampling in two- and one-dimensional domains are related to those for the three-dimensional volume. In general, the sampling in lower-dimensional domains allows us to calculate a lower bound for the volumetric strains, which is expressed as a well-defined fraction of the measured strains. Except for the one-dimensional estimate of the shear strain, the lower bound defines exactly the volumetric strain if the largest fault in the volume is also the largest fault in the sampled domain.

We derive constraints on the size of the domain that we must use, relative to the size of the largest fault in the analysis, in order to be able to apply the equations for total strain that are based on fault systematics (Eqs. (3.4.2) and (3.4.3)). These limits define the minimum size of the volume that must be included in an analysis of this type for a given maximum-sized fault. Alternatively, the limits prescribe the largest fault that can be included in an analysis of strain that relies on fault systematics for a volume of crust of a given size. Larger faults that cut the domain must be included explicitly by adding their contributions to the strain individually.

Acknowledgements

This research was partially supported by grant DE-FG02-03ER15430 from Chemical Sciences, Geosciences and Biosciences Division, Office of Basic Energy Sciences, Office of Science, U.S. Department of Energy (Marrett). We thank Graham Yielding for helpful comments that have improved the presentation.

Appendix. Supplementary data

Supplementary data associated with this article can be found, in the on-line version, at doi: 10.1016/j.jsg.2010.04.007.

References

Bonnet, E., Bour, O., Odling, N.E., Davy, P., Main, I., Cowie, P., Berkowitz, B., 2001. Scaling of fracture systems in geological media. Reviews of Geophysics 39 (3), 347–383.

Cladouhos, T.T., Marrett, R., 1996. Are fault growth and linkage models consistent with power-law distributions of fault lengths? Journal of Structural Geology 18 (2/3), 282–293.

Clark, R.M., Cox, S.J.D., 1996. A modern regression approach to determining fault displacement–length scaling relationships. Journal of Structural Geology 18 (2/3), 147–152.

Kim, Y.-S., Sanderson, D.J., 2005. The relationship between displacement and length of faults: a review. Earth-Science Reviews 68, 317–334.

Kostrov, V.V., 1974. Seismic moment and energy of earthquakes, and seismic flow of rock. Izvestiya Academy of Sciences USSR, Physics of the Solid Earth 1, 13–21 (English Translation).

Marrett, R., 1996. Aggregate properties of fracture populations. Journal of Structural Geology 18 (2/3), 169–178.

Marrett, R., Allmendinger, R.W., 1991. Estimates of strain due to brittle faulting: sampling of fault populations. Journal of Structural Geology 13, 735–738.

Marrett, R., Allmendinger, R.W., 1992. Amount of extension of "small" faults: an example from the Viking Graben. Geology 20, 47–50.

Marrett, R., Ortega, O.J., Kelsey, C.M., 1999. Extent of power-law scaling for natural fractures in rock. Geology 27 (9), 799–802.

Molz, F.J., Rajaram, H., Liu, S., 2004. Stochastic fractal-based models of heterogeneity in subsurface hydrology: origins, applications, limitations, and future research questions. Reviews of Geophysics 42. doi:10.1029/2003RG000126.

Peacock, D.C.P., Sanderson, D.J., 1993. Estimating strain from fault slip using a line sample. Journal of Structural Geology 15 (12), 1513–1516.

Riznichenko, Y.V., 1965. Seismic Rock Flow, in Dynamics of the Earth's Crust. Nauka, Moscow.

Scholz, C.A., Cowie, P.A., 1990. Determination of total strain from faulting using slip measurements. Nature 346, 837–839.

Twiss, R.J., 2009. An asymmetric micropolar moment tensor derived from a discrete-block model for a rotating granular substructure. Bulletin of the Seismological Society of America 99 (2B), 1103–1131.

Twiss, R.J., Marrett, R. Determining brittle extension and shear strain using fault length and displacement systematics: Part II: Data evaluation and test of the theory. Journal of Structural Geology, in this issue.

Twiss, R.J., Moores, E.M., 2007. Structural Geology, second ed. W.H. Freeman and Co., New York.

Twiss, R.J., Protzman, G.M., Hurst, S.D., 1991. Theory of slickenline patterns based on the velocity gradient tensor and microrotation. Tectonophysics 186, 215–239.

Twiss, R.J., Souter, B.J., Unruh, J.R., 1993. The effect of block rotations on the global seismic moment tensor and the patterns of seismic P and T axes. Journal of Geophysical Research 98 (B1), 645–674.

Walsh, J.J., Watterson, J., 1993. Fractal analysis of fracture patterns using the standard box-counting technique: valid and invalid methodologies. Journal of Structural Geology 15, 1509–1512.

Walsh, J.J., Watterson, J., Yielding, G., 1991. The importance of small-scale faulting in regional extension. Nature 351, 392–393.

Watterson, J., Walsh, J.J., Gillespie, P.A., Easton, S., 1996. Scaling systematics of fault sizes on a large-scale range fault map. Journal of Structural Geology 18 (2/3), 199–214.

Westaway, R., 1994. Quantitative analysis of populations of small faults. Journal of Structural Geology 16, 1259–1273.